

Article

Assessing the Impacts of Climate Change and Water Extraction on Thermal Stratification and Water Quality of a Subtropical Lake Using the GLM-AED Model

Chao Deng ^{1,*}, Hong Zhang ¹  and David P. Hamilton ² 

¹ School of Engineering and Built Environment, Griffith University, Southport, QLD 4222, Australia; hong.zhang@griffith.edu.au

² Australian Rivers Institute, Griffith University, Nathan, QLD 4111, Australia; david.p.hamilton@griffith.edu.au

* Correspondence: chao.deng@griffithuni.edu.au

Abstract: This study combined a catchment model and one-dimensional lake model (GLM-AED) to simulate the response of hydrodynamics and water quality of subtropical Advancetown Lake (South-East Queensland, Australia) to future changing climates from 2040 to 2069 and 2070 to 2099 under Representative Concentration Pathway (RCP) 4.5 and 8.5 and increased water demand from a 50% increase in population over current levels. The simulation adequately reproduced water temperature (RMSE of 0.6 °C), dissolved oxygen (DO) (RMSE of 2 mg/L), and other water quality variables, such as nitrogen, phosphorus, and chlorophyll *a* (Chl-*a*). Warming temperatures dominated the change in thermal structure and hydrodynamic status of the lake under future climate change conditions. Projected changes in precipitation and hydrological response from the upstream catchment might, however, partly offset the warming temperatures under future climate change. Increased water withdrawal due to population growth, which involved water extraction from the epilimnion, showed antagonistic effects on water stability compared to those from climate change. Under a high emission scenario of RCP8.5 during the 2080s, there is an increased likelihood of winter turnover failure in Advancetown Lake. Nutrient concentrations were simulated to decrease from reduced catchment loads under future climate change conditions. However, Chl-*a* concentrations were simulated to increase, especially during the period after winter turnover, under these future conditions. The depth of the hypoxia front during stratification is expected to decrease and move towards the water surface, attributable to the warming water temperatures and prolonged thermal stratification, which might affect biogeochemical processes and exchange fluxes between the hypolimnion and bottom sediments. These potential changes may present challenges for water resource management under future conditions of climate change and population growth.

Keywords: GLM-AED; climate change; thermal stratification; water extraction; lake modelling



Citation: Deng, C.; Zhang, H.; Hamilton, D.P. Assessing the Impacts of Climate Change and Water Extraction on Thermal Stratification and Water Quality of a Subtropical Lake Using the GLM-AED Model. *Water* **2024**, *16*, 151. <https://doi.org/10.3390/w16010151>

Academic Editor: Maria Mimikou

Received: 7 November 2023

Revised: 19 December 2023

Accepted: 25 December 2023

Published: 30 December 2023



Copyright: © 2023 by the authors. Licensee MDPI, Basel, Switzerland. This article is an open access article distributed under the terms and conditions of the Creative Commons Attribution (CC BY) license (<https://creativecommons.org/licenses/by/4.0/>).

1. Introduction

Artificial lakes are of importance in flood mitigation, agricultural irrigation, and water supply [1]. Lakes are sensitive to climate [2], with lake water quality generally considered to be most affected by changes in land use from the upstream catchment and secondarily by climate-induced changes [3–5]. Assessing these potential future impacts on lakes can increase our scientific knowledge of these systems and support policymaking and consequent actions for water resource management and conservation.

The temperature of lake water is strongly affected by meteorological conditions, including short-term variability [6,7]. Water temperature affects other water quality indicators and ecological processes, such as the growth of microorganisms and phytoplankton [8,9], the saturation concentration of dissolved oxygen (DO), and the mineralization rate of organic matter [10]. The vertical temperature profile determines the intensity of thermal

stratification in the water column [11]. During thermal stratification, hypolimnetic DO is depleted by microbial consumption, and the released nutrients from the sediments accumulate in the hypolimnion [12–14].

The mixing process in lakes is induced by the breakdown of stability caused by high wind speeds, convective motions driven by surface water cooling, or physical disturbance of the water column by heavy precipitation events [15,16]. Winter mixing is the dominant water column transport mechanism for monomictic lakes, and mixed lakes have higher nutrient concentrations in the surface waters and higher DO concentrations in the bottom waters after vertical exchange [17].

Stratified waters are more conducive to supporting proliferations of harmful algae such as cyanobacteria, making them more dominant in these waterbodies [18,19]. Warming water temperatures intensify the vertical stratification but reduce water viscosity, further enhancing the competitive advantage of buoyant cyanobacteria over sinking diatoms [18]. Cyanobacteria blooms can increase the surface water temperature locally [20], which in turn is beneficial for them to maintain their competitive advantage over eukaryotic phytoplankton [21].

Global warming from climate change is expected to increase surface water temperature and prolong the duration of summer thermal stratification, increasing the frequency and duration of anoxic conditions in the hypolimnion and thus affecting biochemical responses [22–24]. The in-lake effect, driven by extreme weather conditions, may have a duration that persists well beyond the duration of the event itself [25]. Heavy precipitation events are often accompanied by massive nutrient loads from upstream catchments [6,26]. The increase in precipitation intensity may reset the seasonal plankton community [27]. Warming temperatures, variable nutrient loads, and extended hydraulic retention time may alter the trophic status of lakes and the species composition of the phytoplankton community, as well as the duration of the blooms [3,9,15,28,29].

Water withdrawn for public supply or environmental flows can not only affect the thermal structure of the water column [30,31] but also the DO distribution and duration of anoxia in the hypolimnion [7]. In addition to enhanced thermal stability of the water column, increased water extraction affects the exchange flux of DO and nutrients between the epilimnion and hypolimnion [32], the nutrient release from bottom sediment [29], and the growth of phytoplankton [33]. The flow downstream of dammed lakes is controlled by the amount of water discharged and the depth of offtake of the water from the dam [34,35]. The response of the downstream river system to warming air temperatures depends on changes in the thermal structure of the upstream dammed lake under future climate change conditions [36] and the meteorological conditions directly affecting the river.

There are few assessments that link climate, catchment, and lake models to assess the ecosystem-scale hydrodynamics and water quality responses of lakes to climate change, including responses to catchment inputs [29]. Few assessments have further considered the social impact of increasing water extraction with population growth. The aim of this study was to assess the impact of future warming temperatures, the resulting catchment hydrological response, and the effects on hydrodynamics and water quality of a dammed lake in a subtropical area. This study sought to better understand the impact of climate change and an increase in water demand due to population growth on lake responses by comparing the contributions of these factors under future conditions.

2. Material and Methods

2.1. Study Area

Advancetown Lake (28.051° S, 153.282° E, Figure 1) is located in the hinterland of the Gold Coast in the South-East Queensland (SEQ) region of Australia in a subtropical climate. This lake covers a surface area of 15 km² and has a full supply capacity of approximately 311 Mm³ at 60 m depth after the third upgrade in 2011. The lake has two tributaries, the Nerang River and the Little Nerang Creek, with a total upstream catchment area of 207 km². The lake serves as an important potable water supply within the water supply grid of the

SEQ region. The average daily water extraction was around 126 ML based on the period of July 2011–December 2019. A minimum release of 7250 m³/d is required to maintain aquatic ecosystem health in the downstream Nerang River. The mean residence time of the lake was doubled from 2.5 years prior to the upgrade to 4.9 years since the 2011 upgrade [37].

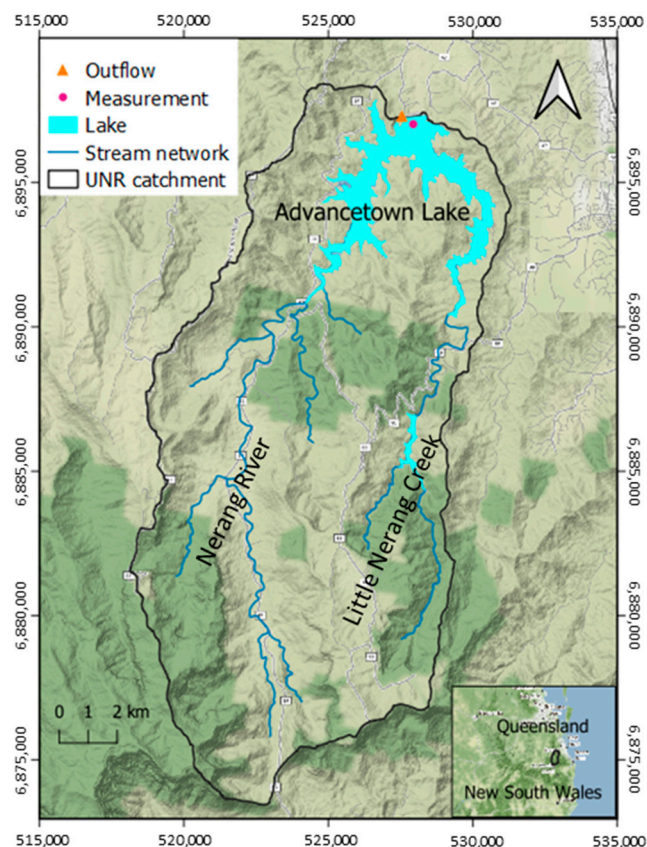


Figure 1. Location of the Upper Nerang River (UNR) catchment and the water sampling site (Measurement) and spillway (Outflow) of Advancetown Lake. This lake receives inflows from two tributary creeks: the Nerang River on the west and Little Nerang Creek on the east.

2.2. Model Setup and Inputs

The General Lake Model (GLM) is an open-source 1-D lake hydrodynamic model that uses a Lagrangian layer scheme in the vertical dimension to calculate the distribution of temperature, salinity, and density [38]. A flexible layer routine can automatically allow adjustment of the thickness of the water layer with uniform properties of layers for each simulation step, which can reduce computing requirements and achieve fast and efficient operation. GLM simulates the occurrence of thermal stratification and vertical mixing processes based on the energy balance between the kinetic energy of the water column and the internal potential energy [38]. This model assumes that mixing occurs when the total available kinetic energy contributed by wind stirring, convective overturn, shear production between layers, and Kelvin–Helmholtz (K–H) billowing exceeds the potential energy required to maintain stratification. When the internal kinetic energy is insufficient to overcome the potential energy, the mixing process ends, and the stratification process begins. GLM has successfully been applied to simulate the water temperature distributions in lakes under different elevations, climates, mixing states, and morphologies around the world [39]. The Aquatic EcoDynamics (AED) model simulates a variety of biochemical processes, including inorganic and organic nutrient cycling, oxygen dynamics, and biological organisms [40]. It includes sub-modules such as suspended solids (SS), DO, silica (Si), nitrogen (N), phosphorus (P), organic matter, Chl-*a*, phytoplankton, and zooplankton. Some of the processes simulated include decomposition and mineralization

of organic matter, nitrification and denitrification, nutrient release from bottom sediment, phytoplankton uptake, and organism excretion.

The GLM-AED model requires multiple driving datasets for configuration, including lake morphology, initial water vertical profile, inflow characterized by water temperature and nutrient concentrations, lake outflow, and meteorological data [38]. The morphological data of Advancetown Lake (Figure S1) were provided by Seqwater (<https://www.seqwater.com.au/>, accessed 10 June 2021). Inflow data were derived from the outputs simulated for the Upper Nerang River catchment using a Soil and Water Assessment Tool (SWAT) model [41]. Meteorological datasets, such as precipitation, air temperature, and relative humidity, were downloaded from SILO (<https://www.longpaddock.qld.gov.au/silo/>, accessed 10 June 2021), while solar radiation was available from the Bureau of Meteorology, Australia (<http://www.bom.gov.au/>, accessed 10 June 2021). Cloud cover was derived from solar radiation using the method described by Luo et al. [42]. Wind speed was measured using observations from the southeast Coolangatta airport, 20 km away (source: <https://www.noaa.gov/>, accessed 10 June 2021). Daily water withdrawal for public supply was provided by Seqwater, and a minimum discharge of 7250 m³/d was set as ecological flow to meet current regulations of the City of Gold Coast. As an ungated dam and mimic the gradual water level recession due to flood spill during storm events, a series of virtual pumps were configured at different elevations, and their pumping rates were calculated based on the spillway structure geometry data.

2.3. Model Calibration and Analysis

The Advancetown Lake model was run with daily input data and produced daily outputs for an 8.4-year period, from August 2011, after the third stage of the dam upgrade, to December 2019. The model calibration period was from August 2011 to June 2017, and validation was from July 2017 to December 2019. The GLM-AED model was initialized with the water temperature and DO vertical profiles at 10:00 h, and the water quality modules were initialized with the surface values from the monthly water quality sampling program at the model startup. Parameters and their defaults/ranges used for model calibration are listed in Table 1. The light extinction coefficient (K_w) was set to 0.5 m⁻¹. The objective functions of Pearson product moment correlation coefficient (r) and root-mean square error (RMSE) were used to evaluate the model performance during calibration and validation periods.

Table 1. Calibrated parameters to simulate water temperature, dissolved oxygen, and other chemical parameters in Advancetown Lake using GLM-AED.

Symbol	Description	Range or Default	Assigned Value
Hydrodynamic			
C_k	Mixing efficiency—convective overturn [-]	0.1–0.2	0.14
C_w	Mixing efficiency—wind stirring [-]	0.2–0.3	0.21
C_s	Mixing efficiency—shear production [-]	0.2–0.3	0.29
C_T	Mixing efficiency—unsteady turbulence effects [-]	0.2–0.7	0.56
C_{HYP}	Mixing efficiency—hypolimnetic turbulence [-]	0.4–0.8	0.74
Dissolved oxygen			
Fsed_oxy	Sediment oxygen demand [mmol m ⁻² d ⁻¹]	–100–0	–55
Ksed_oxy	Half-saturation concentration of oxygen sediment flux [mmol m ⁻³]	10–100	100
Nitrogen			
Rnitrif	Maximum reaction rate of nitrification at 20 °C [d ⁻¹]	0.1	0.1
Rdenit	Maximum reaction rate of denitrification at 20 °C [d ⁻¹]	0.3	0.05
Knitrif	Half-saturation oxygen concentration for nitrification [mmol m ⁻³]	80	40
Kdenit	Half-saturation oxygen concentration for denitrification [mmol m ⁻³]	2	30
Fsed_amm	Sediment NH ₄ -N flux [mmol m ⁻² d ⁻¹]	40	3
Ksed_amm	Half-saturation oxygen concentration controls NH ₄ -N flux [mmol m ⁻³]	25	15

Table 1. Cont.

Symbol	Description	Range or Default	Assigned Value
Phosphorous			
Fsed_frp	Sediment PO ₄ -P flux [mmol m ⁻² day ⁻¹]	-	0.05
Ksed_frp	Half-saturation oxygen concentration controls PO ₄ -P flux [mmol m ⁻³]	-	50
Organic matter			
Rpoc_hydrol	Maximum rate of decomposition of particulate organic carbon (POC) at 20 °C [d ⁻¹]	0.01–0.08	0.02
Rdoc_minerl	Maximum rate of aerobic mineralization of labile dissolved organic carbon (DOC) at 20 °C [d ⁻¹]	0.01–0.08	0.08
d_pom	Diameter of particulate organic matter (POM) [m]	-	5 × 10 ⁻⁶
Rpon_hydrol	Maximum rate of decomposition of particulate organic nitrogen (PON) at 20 °C [d ⁻¹]	0.01–0.08	0.08
Rdon_minerl	Maximum rate of aerobic mineralization of labile dissolved organic nitrogen (DON) at 20 °C [d ⁻¹]	0.01–0.08	0.08
Rpop_hydrol	Maximum rate of decomposition of particulate organic phosphorous (POP) at 20 °C [d ⁻¹]	0.01–0.08	0.01
Rdop_minerl	Maximum rate of aerobic mineralization of labile dissolved organic phosphorous (DOP) at 20 °C [d ⁻¹]	0.01–0.08	0.08
theta_hydrol	Temperature multiplier for the temperature dependence of particulate decomposition rate [-]	1	1.04
theta_minerl	Temperature multiplier for temperature dependence of mineralization rate [-]	1	1.08
Fsed_doc	Sediment DOC flux [mmol m ⁻² d ⁻¹]	-	10

rLakeAnalyzer [43] was used to calculate the thicknesses of different layers in the thermal structure and Schmidt stability (S_T , units: J/m²) from the simulation results. S_T represents the strength of stratification, that is, the dynamic stability of the system [44], and its value represents the amount of work required to mix the entire water column to a uniform density. Therefore, a higher S_T value indicates more stable stratification. The water temperature difference between the lake surface and bottom water (20 m deep) exceeding 1 °C is considered a condition of stratification satisfied [45]. Such a concept can also be found in the study of [24]. In the present work, thermal stratification was determined as a 2 °C water temperature difference between the surface water and the layer 20 m above the lake bottom and lasting for more than 96 h, as described in a Brazil study [46].

2.4. Scenarios

Future climate change scenarios (see Table S1) and change factors of precipitation and air temperature are consistent with those applied in the previous hydrological study [41], including two 30-year periods of the ‘2050s’ (2040–2069) and ‘2080s’ (2070–2099) under a medium emission scenario of RCP4.5 (R45 and R48) and a high emission scenario of RCP8.5 (R85 and R88). These changes are based on the dynamically downscaled Coupled Model Intercomparison Project 5 (CMIP5) Global Climate Models (GCMs) against historical observation data [47]. In comparison with a baseline period of 2011–2019, air temperatures are expected to increase by 1.4–3.9 °C and precipitation to increase by 0.7–5.3% under future changing climate conditions (Table S2). The hydrological response of flow and nutrient loads from the Upper Nerang River catchment was simulated by the calibrated SWAT model (Table S2). Future changes in solar radiation and wind speed were not considered in this study because of the high uncertainty in relative changes based on GCM predictions.

The future population of the SEQ region is likely to increase by around 50% by 2041, based on the current condition [48]. Advancetown Lake provides source water for Gold Coast and other cities through the SEQ Water Grid network. Future water extraction may increase by around 50% by 2041, assuming fixed per capita water consumption. We evaluated the responses of hydrodynamics and water quality in Advancetown Lake to:

(i) warming air temperature under future climate change conditions (T), (ii) future climate change and upstream catchment hydrological variations in flow and nutrient loads (CC), and (iii) a 50% increase in water extraction induced by population growth under CC scenarios (CE).

3. Results

3.1. Performance of the GLM-AED Model

Most of the GLM-AED parameters were configured with the default values, and the calibrated parameters controlling the hydrodynamics, dissolved oxygen, and water quality modules are listed in Table 1. As presented in Figure 2, the coupled GLM-AED model simulated the water temperatures and DO profiles with good consistency with the measurements. The model reproduced the thermal stratification during the warm seasons and complete vertical mixing (winter turnover) during the winter in Advancetown Lake. We applied the Pearson correlation coefficient (r), significance (p), and RMSE to evaluate the accuracy of the simulations by the coupled model. The GLM-AED model simulated water temperature with RMSEs of $0.62\text{ }^{\circ}\text{C}$ ($r = 0.970$, $p < 0.01$) during the calibration period from August 2011 to June 2017 and $0.57\text{ }^{\circ}\text{C}$ ($r = 0.980$, $p < 0.01$) during the validation period of July 2017 to December 2019, respectively (Table 2). The model reproduced water temperatures at different depths below the water surface (see Figure 3a), especially for the surface layer at a depth of 2 m with a r value of 0.985 (see Table 2).

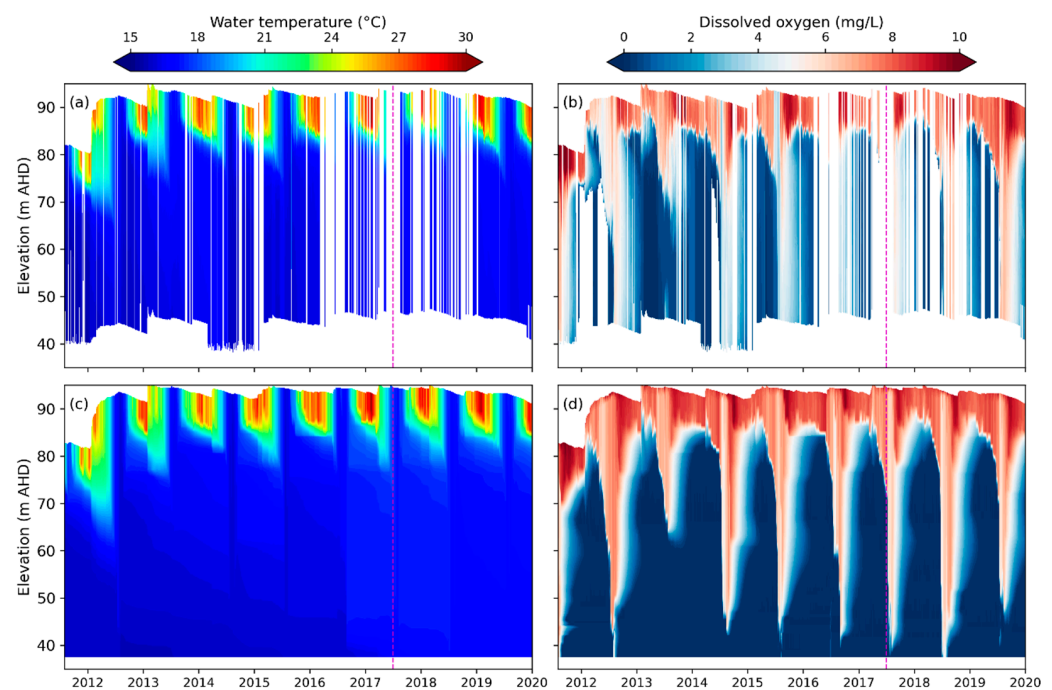


Figure 2. Contour plots of daily measured (a) water temperature and (b) dissolved oxygen concentration interpolated from hourly Vertical Profiling System (VPS) records provided by SEQWater and simulated (c) water temperature and (d) dissolved oxygen concentration reproduced by GLM-AED at Advancetown Lake. The vertical dashed line separates the calibration and validation periods.

The results in Figure 3b indicate good simulation of DO at different depths in the water column, except for overestimates at 2 m depth before thermal stratification and oxygen depletion rates in the hypolimnion (40 m depth) after winter turnover. Overall, the model simulated the DO with a RMSE of 1.63 mg/L ($r = 0.860$, $p < 0.01$) during the calibration period and 2.07 mg/L ($r = 0.755$, $p < 0.01$) during the validation period (see Table 3).

Table 2. Pearson correlation coefficient (r), level of significance (p), and Root Mean Square Error (RMSE) of simulated water temperature ($^{\circ}\text{C}$) and dissolved oxygen (mg/L) at different depths below the water surface and for the whole water column during the calibration period of August 2011 to June 2017 and the validation period of July 2017 to December 2019, respectively, in Advancetown Lake. $^{\dagger} p < 0.01$.

Depth (m)	Water Temperature				Dissolved Oxygen			
	Calibration		Validation		Calibration		Validation	
	r	RMSE	r	RMSE	r	RMSE	r	RMSE
2	0.985 [†]	0.66	0.994 [†]	0.43	0.744 [†]	1.01	0.732 [†]	0.58
10	0.891 [†]	0.98	0.862 [†]	0.96	0.735 [†]	2.20	0.783 [†]	1.75
15	0.934 [†]	0.70	0.946 [†]	0.69	0.806 [†]	1.73	0.821 [†]	1.57
20	0.939 [†]	0.42	0.721 [†]	0.53	0.916 [†]	1.23	0.843 [†]	1.42
40	0.442 [†]	0.32	0.673 [†]	0.50	0.759 [†]	1.49	0.743 [†]	2.11
Overall	0.970 [†]	0.62	0.980 [†]	0.57	0.860 [†]	1.63	0.755 [†]	2.07

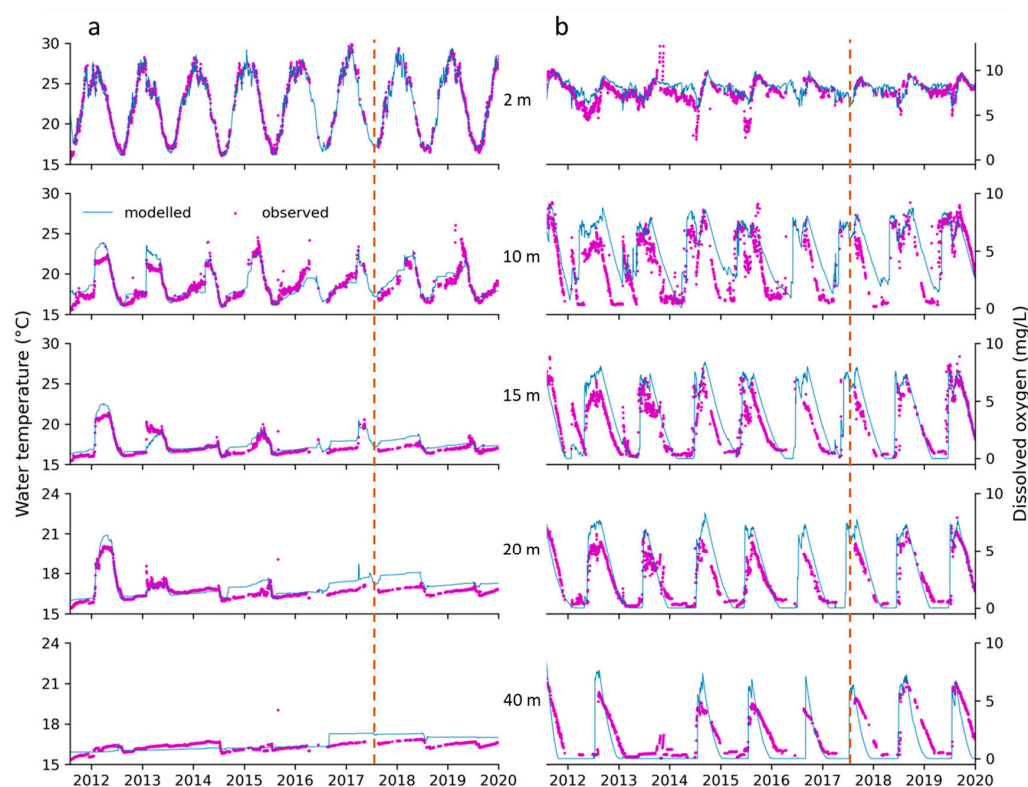


Figure 3. Comparison of modeled (a) water temperature and (b) dissolved oxygen concentration at different depths below the water surface in Advancetown Lake during the calibration period of August 2011 to June 2017 and the validation period of July 2017 to December 2019. The orange vertical dashed line separates the calibration and validation periods.

The GLM-AED model adequately reproduced nutrient concentrations in the surface layer, especially the increase of ammonium concentrations (Figure 4a) during the winter turnover and subsequent increase of nitrate concentrations (Figure 4b) with $r \geq 0.377$ during the calibration period and $r \geq 0.396$ for validation (see in Table 3) in the surface layer. RMSEs for simulated ammonium and nitrate concentrations are less than 0.009 mg/L and 0.032 mg/L, respectively. Concentrations of TN from the surface layer were relatively stable with small interannual variations except for the peak recorded in January 2012, right after the third upgrade. The overall estimated RMSE for TN is less than 0.075 mg/L ($r \geq 0.22$). The phosphorus simulation is less satisfactory with low r values (Table 3),

particularly the negative r value for the phosphate simulation during the validation period. In addition, the model failed to simulate the high phosphorus event (see Figure 4e). The GLM-AED model reproduced the total organic carbon (TOC) concentrations in the surface layer with reasonable accuracy (Figure 4f), with RMSEs less than 0.7 mg/L and r values of 0.486 for calibration and 0.419 for validation, respectively.

Table 3. Model performance of GLM-AED for daily mean concentrations of ammonia (NH₄-H), nitrate (NO₃-N), total nitrogen (TN), phosphate (PO₄-P), total phosphorus (TP), total organic carbon (TOC), and chlorophyll *a* (Chl-*a*) in the surface layer of Advancetown Lake during the calibration period of August 2011 to June 2017 and the validation period of July 2017 to December 2019, respectively. Pearson correlation coefficient (r), level of significance (p), and Root Mean Square Error (RMSE) were used to indicate model performance. * $p < 0.05$, † $p < 0.01$.

Period	Statistics	NH ₄ -H	NO ₃ -N	TN	PO ₄ -P	TP	TOC	Chl- <i>a</i>
		mg/L						μg/L
Calibration	r	0.838 †	0.377	0.326 †	0.212	0.166	0.486 †	−0.244
	RMSE	0.009	0.032	0.075	0.004	0.008	0.686	1.872
Validation	r	0.938 †	0.693 †	0.224	−0.035	0.230	0.419 *	−0.102
	RMSE	0.006	0.020	0.038	0.005	0.005	0.656	0.988

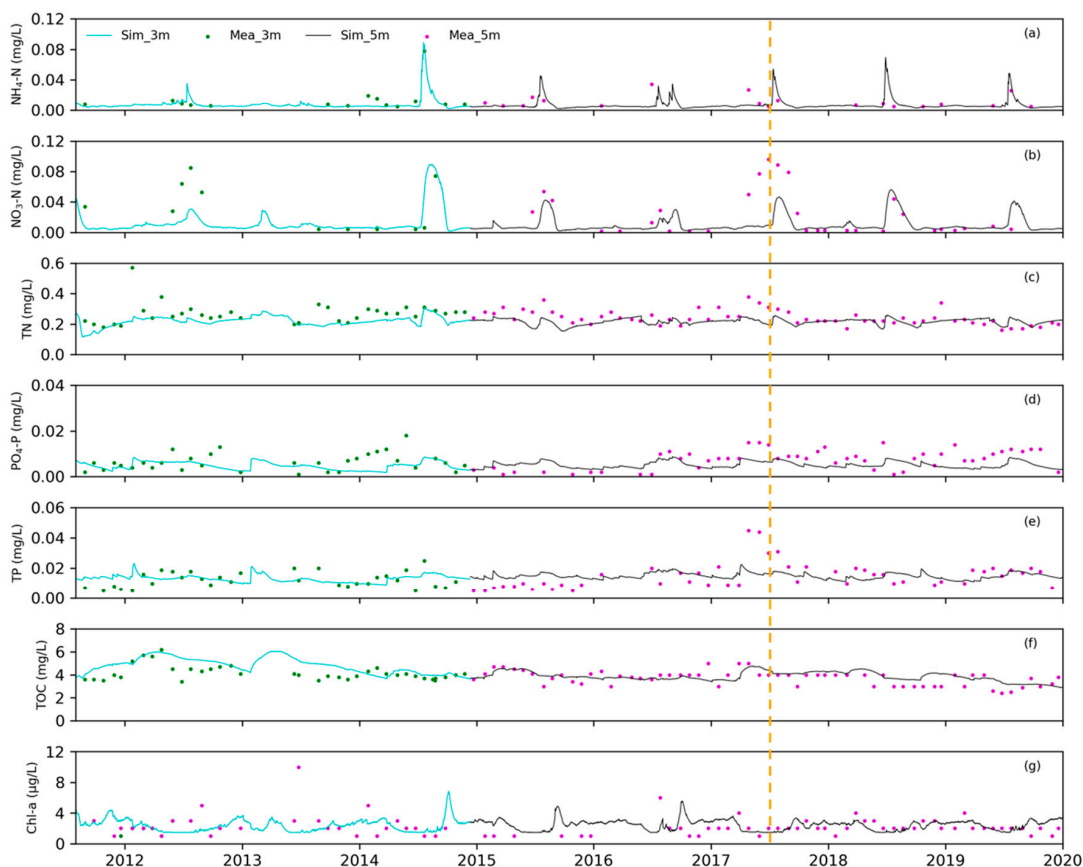


Figure 4. Comparisons of concentrations of (a) ammonium (NH₄-N), (b) nitrate (NO₃-N), (c) total nitrogen (TN), (d) phosphate (PO₄-P), (e) total phosphorus (TP), (f) total organic carbon (TOC), and (g) Chlorophyll *a* (Chl-*a*) simulated by GLM-AED with measurements for the surface layers (3 m and 5 m) of Advancetown Lake during the calibration period (August 2011 to June 2017) and validation period (July 2017 to December 2019), separated by the vertical dashed orange line.

Chl-*a* was mostly at low concentrations in the surface water, except for a high Chl-*a* event during the winter turnover in the year 2013 (see Figure 4g). GLM-AED did not simulate Chl-*a* particularly well, with negative *r* values during both calibration and validation periods.

3.2. Baseline Condition

The thermal structure of Advancetown Lake was simulated by the GLM-AED model over an 8.4-year period from August 2011 to December 2019 (the baseline). The observed and simulated monthly water temperature in the surface layer (0–5 m) ranged from 16.8 to 27.0 °C and from 16.9 to 27.2 °C (Figure 5a), respectively, with the warmest January, which is consistent with the warmest monthly air temperature around the year. The difference in surface temperature is minor (≤ 0.3 °C) between simulation and observation, except for the 0.4–0.5 °C higher for the simulation over observation during the hot February and cold August periods. Monthly temperatures in the hypolimnion (20 m above the lake bottom) varied slightly between 16.1 °C and 16.5 °C in measurements and were simulated to be in the range of 16.6–17.6 °C (see Figure 5b). Water temperatures were overestimated by 1.1–1.2 °C during the autumn season from March to May. This lake showed a monomictic regime characterized by the periodic annual mixing with winter turnover during the period from June to September and the stratification established between October and May (Figure 2). During the stratification periods, the mean thermocline depth ranged from 7.1 m to 15.0 m (Figure 6a), and the thickness of epilimnion (Figure 6b) and metalimnion (Figure 6c) varied from 4.6 m to 14.0 m and from 2.1 m to 5.7 m, respectively. The monthly Schmidt stability index (S_T), derived from the modeled temperature profiles, varied between ~ 40 and 1700 J/m², with a peak in January. S_T remained above 700 J/m² during a well-established stratification event and showed the lowest stability in July and August, when the annual periodic mixing events occur during the winter season. The mean annual thermal stratification duration period is simulated to be 273.5 ± 13.9 d/y, as shown in Figure S2.

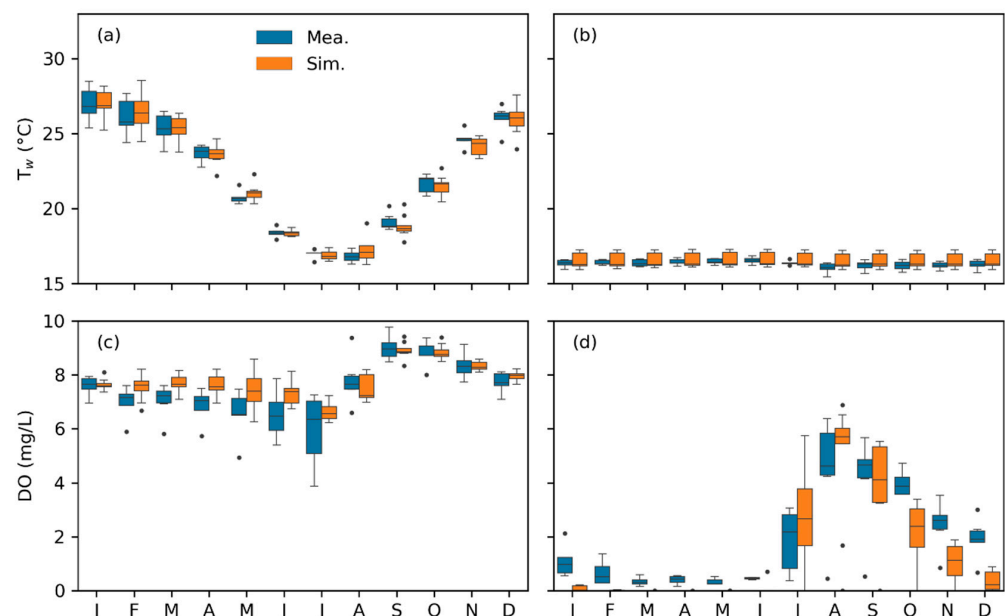


Figure 5. Mean monthly water temperature (T_w) and dissolved oxygen concentrations (DO) in the surface layer (a,c) and hypolimnion (b,d, 20 m above the lake bottom) from measurements and simulations in Advancetown Lake during the baseline period from August 2011 to December 2019. Dots represent statistical outlier values.

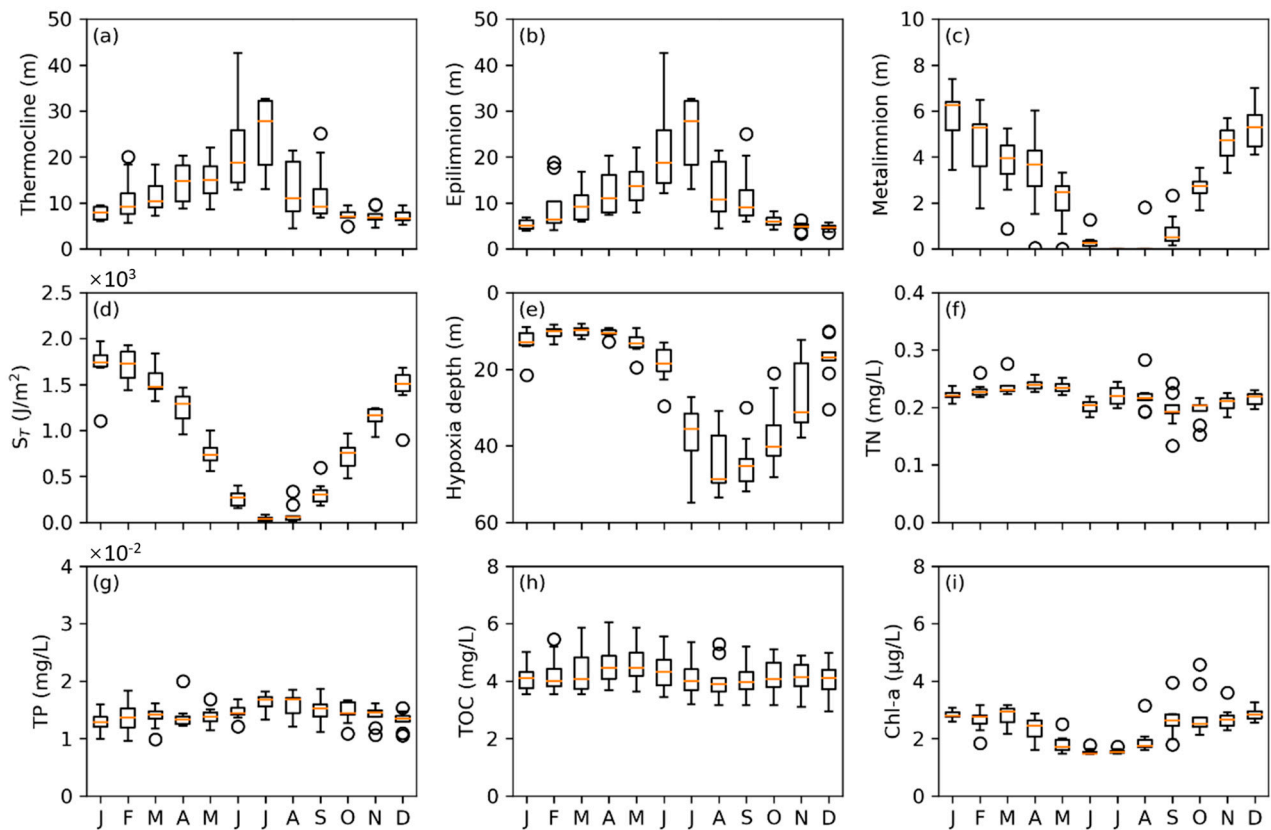


Figure 6. Monthly statistics of thermocline depth (a), thickness of epilimnion (b) and metalimnion (c), Schmidt stability index (S_T , d), depth of hypoxia (e) for Advancetown Lake, and monthly concentrations of total nitrogen (TN, f), total phosphorous (TP, g), total organic carbon (TOC, h), and Chlorophyll-*a* (Chl-*a*, i) in the surface layer during the baseline period. Circles represent statistical outlier values.

Simulated monthly DO varied in the range of 7.8–9.3 mg/L, which is higher than the measurements of 6.0–9.0 mg/L, with the peak in September (Figure 5c) after the winter turnover and the lowest in July. The simulated surface DO is about 0.1–1.9 mg/L higher than measurements with the highest differences (>1 mg/L) during the period from February to July. The peak difference of 1.9 mg/L is found in July in surface water. In the hypolimnion, DO was simulated to be 0–6.4 mg/L, which is a greater variation than 0.3–4.4 mg/L in the measurements. Both simulated and measured DO peaked in August during the winter turnover period (Figure 5d), then gradually decreased during the warm seasons of summer and autumn. During the period from June to September, the simulated DO is about 1.3–3.7 mg/L higher than measurements, with the largest overestimation of 3.7 mg/L in July. During the warm period from December to April, DO was underestimated in comparison to the measurements. The depth of the hypoxia front was derived from the simulated DO profiles using a threshold of 2 mg/L. The monthly averaged hypoxia depth ranged from 10 to 17 m during the warm seasons (Figure 6e) and peaked around 45 m in August during winter turnover.

The nutrient concentrations were simulated to be relatively stable, with range in concentrations of TN (Figure 6f), TP (Figure 6g), and TOC (Figure 6h) of 0.19–0.24 mg/L, 0.012–0.016 mg/L, and 4.0–4.6 mg/L, respectively, with slight intra-annual variations in the surface water. Chl-*a* was simulated to be in the range of 1.5 to 3.0 $\mu\text{g/L}$ (see Figure 6i). TN (Figure 7a) was underestimated in the surface water, but the difference for total phosphorus was smaller (Figure 7b). However, the TOC (Figure 7c) and Chl-*a* (Figure 7d) were overestimated by around 10% in the surface water.

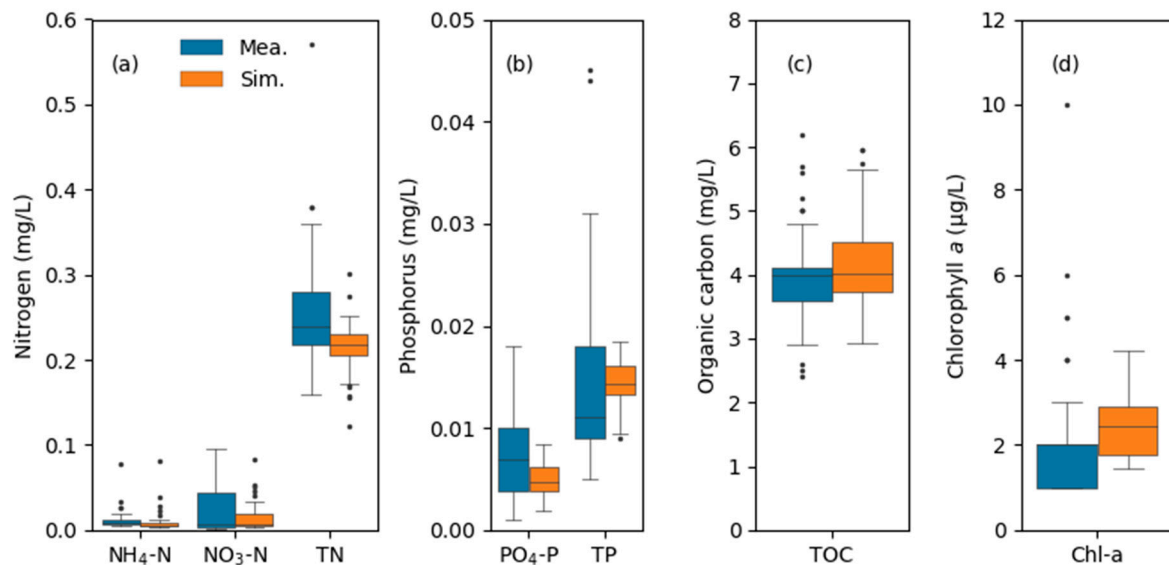


Figure 7. Comparisons of measured and simulated water quality variables of (a) nitrogen (NH₄-N, NO₃-N, and TN), (b) phosphorus (PO₄-P, TP), (c) total organic carbon (TOC), and (d) chlorophyll *a* (Chl-*a*) in surface water from Advancetown Lake during the period of August 2011 to December 2019. Circles represent statistical outlier values.

3.3. Changes in Hydrodynamic Regimes under Future Conditions

3.3.1. Impact of Warming Temperatures (T)

The GLM-AED model was run for future scenarios with updated configurations of climate change and increased water withdrawal from population growth over the reference period from August 2011 to December 2019. The response of the hydrodynamics is shown in Figure 8. Increased water temperatures throughout the water column occurred under future warming air temperatures (Figure 8a–h). Annual water temperature is simulated to increase by 1.1–3.1 °C in the surface layer, which is higher than that in the hypolimnion (1.0–2.3 °C) but lower than the projected changes in air temperature under each future climate change condition (Table S2). Mean monthly water temperature increased most in the surface layer in September (1.2–3.5 °C) after the winter turnover and least in May (1.0–2.8 °C). The smallest increase in the hypolimnion was in the warmest month of January (0.9–2.0 °C). The water temperatures in the surface layer are more sensitive to air temperature changes than in the hypolimnion; that is, the warmer the air temperature, the greater the temperature difference between the surface layer and hypolimnion under future warming conditions.

Under two warming temperature conditions of RCP4.5 (R45-T and R48-T), the thermocline depth is slightly smaller in summer and autumn (see Figure 8i,j). Under R85, the increase in thermocline depth is less than R48. The warmer air temperature condition under R88 resulted in a decrease in thermocline depth to 6 m in June (see Figure 8l). Annual variations for thermocline depth are predicted to be 1.4 m, 1.3 m, −0.5 m, and −1.7 m, respectively, under the four future warming scenarios of R45-T, R48-T, R85-T, and R88-T. The greatest decrease in thermocline depth was around 6 m in June under the R88 temperature (R88-T) scenario (see Figure 8p). The annual mean epilimnion thickness changes in the range of −1.8–1.5 m under the four warming temperature conditions. The metalimnion thickness is estimated to decrease by 0.5–1.2 m in January (Figure 8q–t) and to increase by up to 0.9 m in September and October under future warming temperature conditions (Figure 8t). Under future warming scenarios, an overall increase in the Schmidt Stability Index (S_T) is predicted more in warm seasons than in cold seasons (Figure 8u–x). Increases in S_T are predicted to be lowest, about 50 to 260 J/m², in July and highest, 110–440 J/m², in January. Thermal stratification periods are prolonged under future warming conditions (Figure S2), with changes of 13.9 d/yr, 19.5 d/yr, 27.4 d/yr, and 63.8 d/yr under scenarios R45-T, R48-T, R85-T, and R88-T, respectively. Under the scenario of R88-T, the vertical

mixing process in winter is greatly weakened with increasing risk of consecutive thermal stratification over a period of several years.

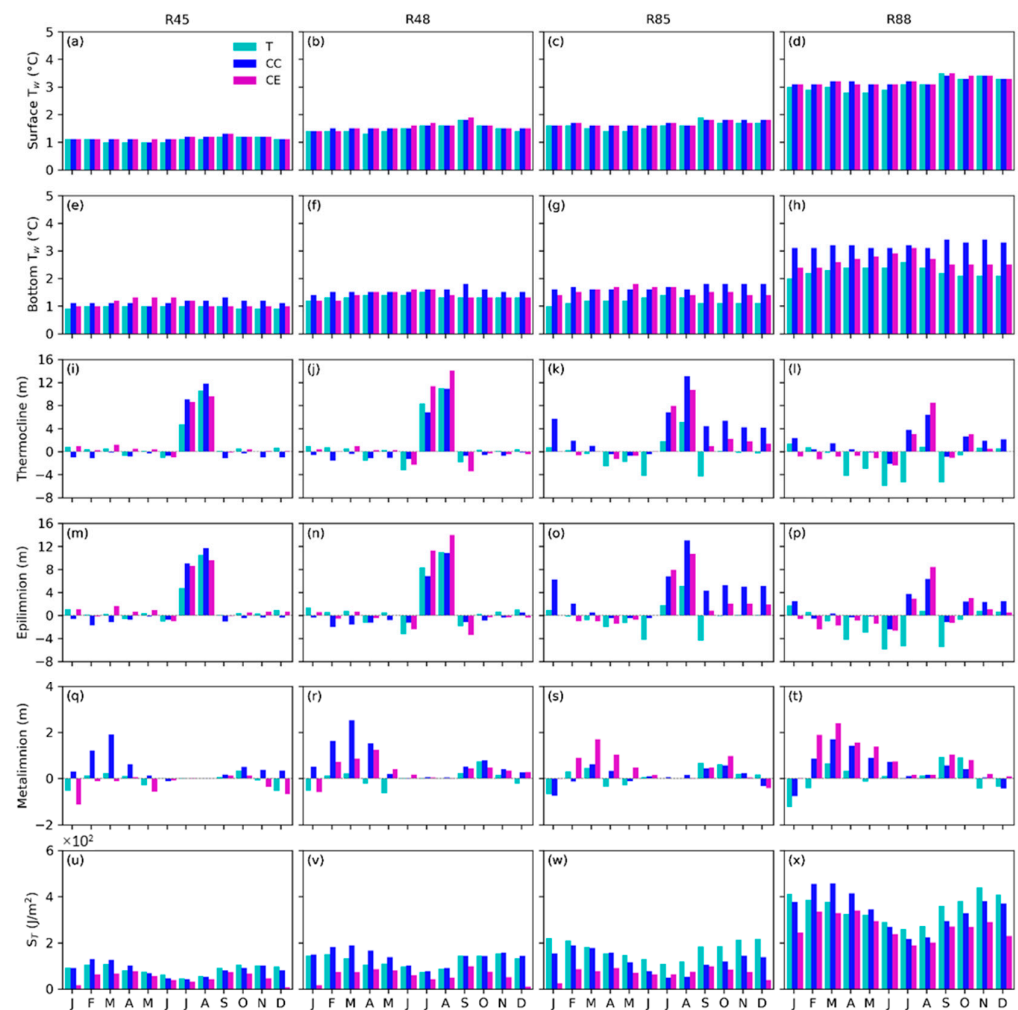


Figure 8. Predicted monthly changes in water temperatures (T_w) of the surface layer (a–d) and hypolimnion (e–h), thermocline depth (i–l), thickness of epilimnion (m–p) and metalimnion (q–t), and Schmidt stability index (S_T , u–x) in Advancetown Lake under different conditions of warming temperatures (T), climate change (CC), and increasing water extraction (CE) over the baseline period of August 2011 to December 2019.

3.3.2. Impact from Climate Change (CC)

Under climate change scenarios, rainfall and upstream catchment hydrological response affect inflows to Advancetown Lake, including discharge, temperature, and sediment and nutrient loads. Water temperature is predicted to increase by 1.1–3.2 °C in the surface layer and by 1.1–2.8 °C in the hypolimnion under warming scenarios. The maximum temperature increase in the hypolimnion is simulated to occur in April with a value of 1.2 °C from R45-CC (see Figure 8a), which is different from the scenario of R45-T. Comparatively, the water temperature is further increased by around 0.1 °C in the surface layer and by 0.2–0.9 °C in the hypolimnion, under CC scenarios compared with the temperature scenarios. Changes predicted in thermocline depth and epilimnion thickness are similar under CC scenarios to those from temperature scenarios, i.e., the peak increases are in the period of July and August. Under the future emission scenario of RCP4.5, these changes have significant monthly increases of 9.1–11.8 m and 6.9–10.9 m for thermocline depth and epilimnion thickness, respectively, during July and August, but with declines of varying magnitude in the remaining period. Under climate change scenarios of RCP8.5, the

thermocline depth and epilimnion thickness tend to increase during the warm period from November to March. Under future emission conditions of RCP4.5, smaller magnitudes of annual thermocline depth and epilimnion are predicted from CC scenarios than those under warming air temperature conditions, while they are in the opposite direction under future emission conditions of RCP8.5. Nevertheless, metalimnion thickness is estimated to increase during the autumn season, with the greatest increases from 0.6 m to 2.5 m in March (see Figure 8q–t). Compared to warming temperature conditions, the predicted metalimnion thickness is greater before the winter turnover period under the CC condition, except for the R85-CC scenario. S_T increases in the lake are lower after winter turnover but greater during the period from February to April (except for R48-CC) under CC scenarios in comparison with those for the temperature scenarios. The monthly S_T peaks in February or March, with values between 130 J/m² and 460 J/m² under CC scenarios. Thermal stratification duration is prolonged by 11.1–56.1 day/yr over the baseline (see Figure S2), but decreased in comparison with the warming temperature scenarios, except for the R48-CC scenario, which has a slightly longer duration of 0.8 day/year than the R48-T scenario.

3.3.3. Impact from Climate Change and Increased Water Withdrawal (CE)

Under the CE condition of coupling climate change (CC) with a 50% increase in water extraction (WE) from the lake, the relative changes in water temperature are similar to those of the CC scenarios, which are relatively minor in the surface layer but greater in the hypolimnion compared with the CC scenarios. The increasing water extraction can partly offset the increases in water temperature in the hypolimnion under CC scenarios during the period from August to February, especially for the R88 scenario, with water temperature in the R88-CE lower than that of the R88-CC by as much as around 1 °C. The changes in water temperature in the hypolimnion under CE scenarios are similar to those of RCP4.5, but for RCP8.5, they are around 0.4 °C warmer. The increasing water extraction for CE scenarios inhibits the expansion of the metalimnion layer that occurred in CC scenarios. Annual S_T in CE scenarios is smaller than for both T and CC scenarios (Figure 8u–x). It can be clearly seen that increasing water extraction from CE significantly offsets the increases in S_T brought by changing climatic conditions (T or CC), but S_T is higher in July and August in R85-CE than in R85-CC. The thermal stratification period in CE scenarios is 11.4–50.3 days/year longer than in the baseline condition (see Figure S2). Compared to CC, increasing water extraction in CE tends to further prolong the thermal duration by 0.3 d/yr and 3.9 d/yr during the 2050s but shorten it by 7.4 d/yr and 5.9 d/yr during the 2080s for RCP4.5 and RCP8.5, respectively.

3.3.4. Impact on Epilimnetic Water Quality

Future warming air temperatures are likely to reduce the dissolved oxygen (DO) concentrations in surface waters, but with small changes (see Figure 9a–d). The estimated highest annual DO reduction would be within 4% of the baseline under the high emission condition of R88. Future temperature scenarios would likely result in higher TN concentrations in surface water during the period from October to January after winter turnover. Specifically, the TN changes are predicted to be less than 10% under projected temperature conditions from the RCP4.5 emission scenarios, but to be around 18% and 10% in October during the 2080s under conditions of R48-T and R88-T. In June, before the pre-winter turnover, TN concentrations were estimated to have experienced significant increases, especially a 25% increase under the R48-T scenario over the baseline condition. It is worth noting that the monthly TN concentrations are expected to increase by 7%–25%, with an overall annual increase of 12% under the R48-T scenario (Figure 9f). TP concentrations are simulated to decrease by 5%–18% in the annual value under three warming temperature conditions: R45, R85, and R88. The most significant decrease is expected to be 22% in November under the R88-T scenario (see Figure 9l). While the TP concentrations are expected to increase, similar to TN, with a peak monthly change of around 28% in June and an annual change of 12% under R48-T (Figure 9j), Chl-*a* concentrations have been

simulated to increase by 5%–12% in the mean annual values under warming temperature conditions compared to the baseline, but the monthly changes vary (c). Simulated Chl-*a* concentrations are expected to increase significantly (up to 15%) during the late winter mixing period by the 2050s. During the 2080s, the estimated Chl-*a* peaks in April, in the autumn season, with increases of 11% for R48-T and 23% for R-88-T, respectively.

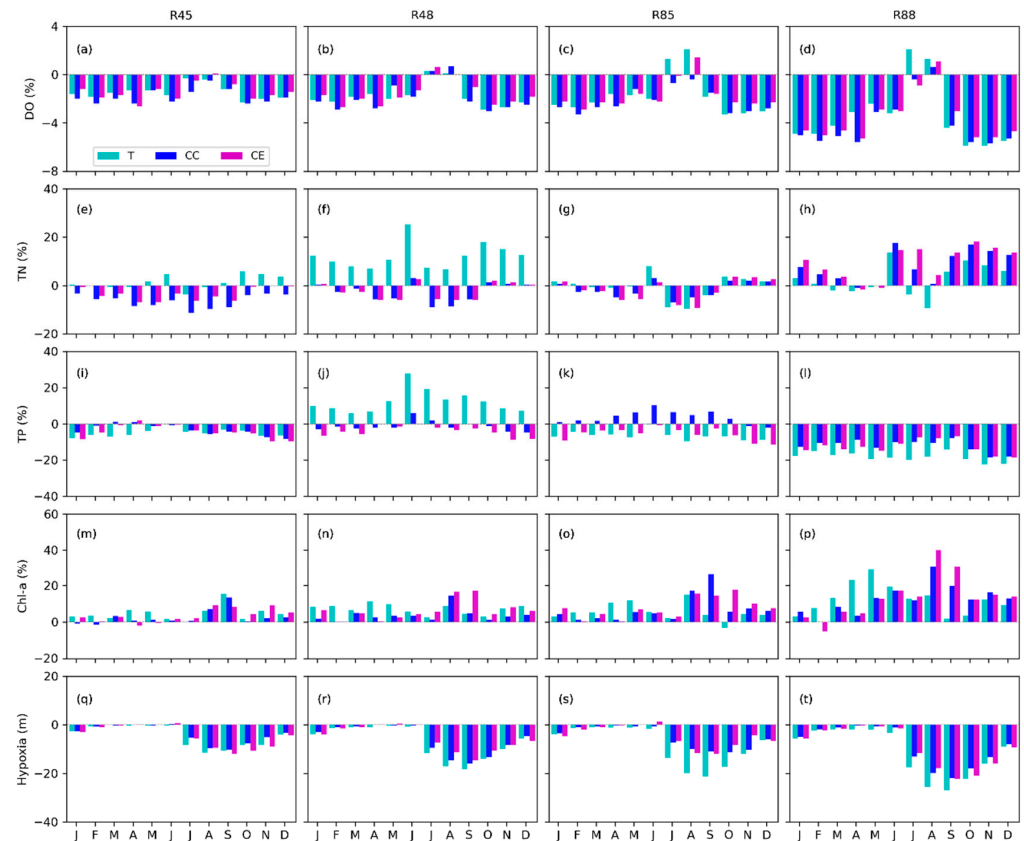


Figure 9. Predicted monthly changes in chemical variables of dissolved oxygen (DO, a–d), total nitrogen (TN, e–h), total phosphorus (TP, i–l), and chlorophyll *a* (Chl-*a*, m–p) in surface water and the depth of hypoxia front (q–t) in Advancetown Lake under different conditions of warming temperatures, climate change, and increasing water extraction over the baseline period of August 2011 to December 2019.

DO concentrations in surface water under CC scenarios are expected to have similar trends to those under the warming temperature scenarios. Mean annual TN concentrations are estimated to decrease by 7% under R45-CC and 3% under R48-CC. The maximum decreases are expected to occur in July during the winter turnover period, with variations of −12% and −9% for the abovementioned scenarios, respectively (see Figure 9a,b). Comparatively, the increases in annual and monthly TN concentration from the R48-CC scenario are much smaller than those from the R48-T scenario. Variations in monthly TN concentrations range from −7% to 3% under the R85-CC scenario, with an annual change of 2%. While these variations are larger than the R88-CC scenario, with monthly values over 12% during the period of June and from September to December (Figure 9h) and an overall annual change of 8% over the baseline. Simulated TP concentrations are expected to decline by around 3% and 1% under R45-CC and R48-CC, respectively, in comparison to concentrations for the baseline. TP concentration is expected to increase under the scenario of R85-CC, particularly in June during the winter mixing period, with monthly changes of 10%. However, TP is simulated to decline significantly under the scenario of R88-CC, with monthly changes ranging from −18% to −8% (Figure 9l). Overall, the annual mean TP concentrations are estimated to increase by 4% under R85-CC while decreasing by 12%

under R88-CC. Predicted variations in annual Chl-*a* concentrations are in the range of 2%–13% under CC scenarios, which are positively correlated with the projected increase in air temperatures listed in Table S2. Nevertheless, the largest monthly increases are in August or September (13–31%), during or after the winter mixing.

Generally, the impacts on surface water quality in Advancetown Lake from the CE scenarios are similar to those from the CC scenarios. Annual mean DO concentrations are estimated to decline by 1–4% under these CE scenarios. Annual mean TN concentrations vary between –2 and 9% under CE scenarios, with higher TN concentrations than those in CC scenarios, except for the R85-CE scenario, which has a lower TN concentration compared with the R85-CC scenario. A decline of 4–13% is expected for TP concentrations in CE scenarios, and these TP concentrations are lower than those from CC scenarios, especially under the R85-CE scenario, declining from 4% under R85-CC to –6% over the baseline. A 4–14% increase in annual Chl-*a* concentrations in surface water is predicted for the CE scenarios over the baseline. It should be noted that during the 2050s, the relative increases of monthly Chl-*a* concentrations in the cold months of August and September were not as high for the CE scenarios as those for the CC scenarios, but during the period from October to January, the CE scenarios had higher Chl-*a* than the CC scenarios (Figure 9m,o). During the 2080s, greater relative changes of monthly Chl-*a* concentrations are expected in the period of August and September from the CE scenarios; up to 17% for R48-CE and 40% for R88-CE compared with the respective CC scenarios (Figure 9n,p).

3.3.5. Impact on Hypoxia

The results show that the hypoxia front, the depth below the water surface derived from the simulated DO profiles with a threshold of 2 mg/L, will move toward the water surface under future warming conditions (Figure 9q–t). The most significant monthly changes are expected during the period from July to November within the winter and spring seasons when the hypoxia front moves 5.2–11.5 m, 10.1–18.3 m, 12.1–21.2 m, and 16.0–27.0 m towards the lake surface under four warming air temperature conditions, respectively, in comparison with the baseline. The largest monthly change is expected to occur in August or September under each temperature scenario. While the monthly changes in hypoxia front depth are relatively modest during the period from February to June, it should be noted that under scenarios with projected higher temperatures, the distance that the hypoxia front moves towards the surface compared with the baseline is a distance of 0.6–4.1 m under the R45-T scenario (Figure 9q) and 2.3–8.9 m under the R88-T scenario (Figure 9t) during the hot summer months from December to February. The mean annual distance that the hypoxia front moves toward the water surface varies from 4.6 m to 11.1 m under future warming temperature conditions. Comparatively, the estimated changes in annual hypoxia front depth under CC scenarios are smaller than those from warming temperature scenarios, ranging from –3.8 m to –8.7 m. These differences between the CC scenario and the warming temperature scenario are mostly in mid and late winter and at the beginning of spring. The greatest difference occurs under the changing climate condition of R85, where the depth for the R85-CC scenario is about 6.1–10.3 m less than for the R85-T scenario during the period from July to October. The response of hypoxia front depth to increasing water extraction under future climate conditions varies in that the hypoxia front moves further toward the surface during the period from September to January in scenarios R45-CE and R88-CE than in the corresponding R45-CC and R88-CC scenarios, with a maximum movement upwards of 3.8 m for R45-CC and 3.1 m for R88-CC, respectively. Comparatively, the distance moved toward the surface in the months of July and August is smaller in CE scenarios than in CC scenarios for the 2080s. Overall, the movement of the mean annual hypoxia front toward the water surface varies from 4.6 m to 9.2 m among these CE scenarios.

3.4. Contributions of Warming Temperatures under Climate Change Conditions

To illustrate the importance of each factor in contributing to the hydrodynamics and water quality in Advancetown Lake, we compared the changes in hydrological inputs from rainfall and the upstream catchment over a warming temperature under climate change conditions and the effect of increasing water extraction over the overall CCs effect, separately. These ratios (shown in Table 4) are categorized into 4 groups to illustrate the strong offset (<−1), antagonistic (−1 ~ 0), synergistic (0 ~ 1), and dominant (>1) effects between the factors. The results show that the input variation would slightly impact surface T_w and enhance warming temperature of the hypolimnion T_w under future climate change scenarios, except for the R48 scenario. Variation in stream inputs offset the impact of warming in reducing thermocline depth and epilimnion thickness, especially for the high emission condition of RCP8.5. A strong antagonistic effect was found for the change in metalimnion thickness under the RCP4.5 emission scenario. While the variation in stream inputs is simulated to increase metalimnion thickness under the climate change condition of R88, it partly offset the impact of warming temperatures under the climate change condition of R85, while it slightly reduced DO concentration in surface water. The stream input changes reduced the impact of warming temperatures on surface TN concentration under the emission scenario of RCP4.5 but strongly increased surface TN for scenario RCP8.5. While an offsetting effect on TP changes is predicted for input variations over warming temperatures, especially under the climate change scenarios of R48 and R85, there is an antagonistic effect under the RCP4.5 emission scenario. A synergistic effect was found on surface Chl-*a* for input variation with warming temperatures of the RCP8.5 emission scenario. Nevertheless, the input variation appeared to offset the influence on hypoxia front depth and thermal stratification duration from warming temperatures under future climate change conditions.

Table 4. Ratios of changes induced by rainfall and upstream catchment hydrological outputs (CC-T) compared with a temperature increase baseline (T-Baseline), and from increasing water extraction (CE-CC) over changing climate (CC-Baseline) under future climate change scenarios. * Mean metalimnion thickness is accounted for during the thermal stratification period.

Variable	(CC-T)/(T-Baseline)				(CE-CC)/(CC-Baseline)			
	R45	R48	R85	R88	R45	R48	R85	R88
Surface T_w	Yellow	Yellow	Yellow	Yellow	Yellow	Yellow	Green	Yellow
Bottom T_w	Yellow	Yellow	Yellow	Green	Green	Green	Green	Green
Thermocline depth	Green	Green	Blue	Blue	Yellow	Red	Green	Green
Epilimnion thickness	Green	Green	Blue	Green	Yellow	Red	Green	Green
Metalimnion thickness *	Blue	Blue	Blue	Green	Blue	Green	Blue	Blue
S_T	Green	Yellow	Green	Green	Green	Green	Green	Green
Surface DO	Yellow	Yellow	Yellow	Green	Green	Green	Green	Green
TN	Blue	Blue	Red	Red	Green	Green	Yellow	Yellow
TP	Green	Blue	Blue	Green	Yellow	Red	Blue	Yellow
Chl- <i>a</i>	Green	Green	Yellow	Yellow	Yellow	Red	Yellow	Yellow
Hypoxia front depth	Green	Green	Green	Green	Yellow	Green	Green	Yellow
Stratification duration	Green	Yellow	Green	Green	Yellow	Yellow	Yellow	Green
Color scale			<−1	−1–0	0–1	>1		

Under future climatic conditions, increasing water extraction would result in little change in T_w in surface and bottom waters. For thermocline depth and epilimnion thickness, increasing water extraction may enhance variations under emission scenario RCP4.5 but offset them under emission scenario RCP8.5.

Offsetting effects are found on S_T and surface DO from increasing water extraction under future climatic conditions. For surface TN concentrations, antagonistic effects from water extraction occur under RCP4.5 but synergistic effects occur under RCP8.5. For TP concentration changes, strong enhancement occurs with water extraction for R48 but a

significant reversal occurs for R85. Extraction enhances the influence of CC on surface Chl-*a* concentration under future climate scenarios. It is noted that for thermal stratification duration, there is a synergistic effect during the 2050s but an antagonistic effect during the 2080s with increasing water extraction relative to climate change. However, changes in hypoxia front depth and thermal stratification duration from increasing water extraction are minor in comparison with those from changing climate.

3.5. Impact of Water Supply Extraction

We examined the effect of a 50% increase in water extraction under a baseline (current) climate and under four different climate scenarios (R45, R48, R85 and R88) on the hydrodynamics and water quality variables in Advancetown Lake relative to a baseline, as shown in Table 5. There is little impact on the surface T_w from increasing water extraction. However, for the hypolimnion T_w , there is an increase of 0.1 °C from the baseline condition, little difference for the R45 scenario, an increase of 0.1 °C for the R85 scenario, but a decrease of 0.1 °C for the R88 scenario. Increasing water extraction would extend the thermocline depth and epilimnion thickness but reduce the thickness of the metalimnion. The increasing water extraction would further increase these changes under climate change, as shown in the R45 scenario compared with the baseline condition, but the situation would be reversed for the R85 emission scenario, i.e., decreased thermocline depth and epilimnion thickness but extended metalimnion thickness. Increasing water extraction is expected to decrease S_T under all climate scenarios, especially during the 2080s. The impact of increasing water extraction on DO concentration is minor in the surface water, as is the impact on TN concentration under the three combined water extraction and climate scenarios of R48, R85, and R88. For the baseline and R45, increasing water extraction would slightly increase the TN in surface water, by 2.2% and 3.1%, respectively. TP concentration is estimated to increase by 2.2% from increasing water extraction in the baseline case, but decrease under future combined water extraction and climatic conditions, with the most significant decrease of −8.9% under the R85 scenario. Chl-*a* concentrations are expected to increase by less than 5% with increasing water extraction, regardless of the climatic conditions. As opposed to the changes in surface DO, increasing water extraction and climate change reduced the depth of the hypoxia front, except for an increase in the R48 scenario. The decrease is about 1.2 m under the water extraction baseline case, while absolute changes are within 0.5 m under the climate change scenarios. The impact of increasing water extraction on thermal stratification duration varies among climate scenarios. It is predicted to reduce the duration by 0.5 d/yr under the baseline condition but to further extend the duration by 0.3 d/yr and 3.9 d/yr under scenarios R45 and R85 during the 2050s. For the 2080 scenarios of R48 and R88, increasing water extraction would reduce the duration by 7.4 d/yr and 5.9 d/yr, respectively.

Table 5. Changes in hydrodynamics and water quality variable concentrations caused by a 50% increase in water extraction in comparison with the corresponding climate scenario under current conditions (WE) and future climate change conditions (R45, R48, R85 and R88) for Advancetown Lake.

Variable	WE	R45	R48	R85	R88
Surface T_w (°C)	0.0	0.0	0.0	0.0	0.0
Bottom T_w (°C)	0.1	0.0	0.0	0.1	−0.1
Thermocline depth (m)	0.4	0.6	0.9	−1.9	−1.0
Epilimnion thickness (m)	0.6	0.8	0.9	−2.1	−0.9
Metalimnion thickness (m) *	−0.4	−0.9	−0.3	0.5	0.7
S_T (J/m ²)	−56	−36	−80	−53	−75
Surface DO (%)	0.6	0.4	0.3	0.5	0.4
TN (%)	2.2	3.1	0.4	−0.4	1.4
TP (%)	2.2	−1.1	−2.8	−8.9	−0.6
Chl- <i>a</i> (%)	4.3	3.2	3.3	2.7	4.9
Hypoxia depth (m)	−1.2	−0.5	0.5	−0.3	−0.4
Stratification (day/year)	−0.5	0.3	−7.4	3.9	−5.9

* Mean metalimnion thickness refers to the thermal stratification period.

4. Discussion and Conclusions

4.1. Model Uncertainty and Limitations

The application of the coupled GLM-AED model in Advancetown Lake has shown good performance, and the overall accuracy of the modelled water temperature ($RMSE \leq 0.62$ °C) is better than in many application cases worldwide ($RMSE$ varying in 0.72–2.14 °C) [39]. A recent study showed the average $RMSE$ of temperature simulation by GLM during the calibration period and the verification period was 1.49 °C and 1.65 °C, respectively, for tropical reservoirs of different sizes in Brazil [46]. The $RMSE$ of the water temperature simulation from this current study is less than that for applications of GLM for lakes in Africa and Europe [7,35,49].

The 1D model does not have the capability to reproduce the horizontal spatial variation in elongated or dendritic waters, and 2D or 3D models are required to capture horizontal advection and dispersion. The hydraulic retention time of the upgraded Advancetown Lake is about 5 years, and the distance between the inlet of the upstream tributary and the outlet of the reservoir exceeds 6 km. The average flow velocity caused by inflow in the longitudinal direction of the lake is much smaller ($\ll 1$ cm/s) than that caused by wind [35]. Therefore, the horizontal spatial variation caused by the inflow was ignored for simulating the water quality near the dam wall of Advancetown Lake [50].

The default setting of GLM ignores the contribution of free convection to evaporative heat flux [38], assuming that evaporative heat flux is proportional to wind speed. However, this is usually considered to underestimate lake evaporation under warm climate conditions [35,51]. The light extinction coefficient, K_w , was set to a constant value of 0.5 m^{-1} in this work, which ignores seasonal changes and may lead to poor predictions for the thermocline in particular [39]. The lake hydrodynamics, especially thermal stratification, are very sensitive to wind speed [2], and the importance of wind speed increases with decreasing water depth [32]. The wind speed dataset in this study was collected from the Coolangatta Airport at a lower altitude than the lake site, about 25 km away, which cannot fully represent the temporal and spatial differences due to terrain differences. Therefore, improving the local meteorological data monitoring will help to further improve the stability of the model.

Selective water withdrawal is a commonly used method during reservoir operation to control the thermal regime of downstream rivers and reservoir water columns [7]. The water intake height in the reservoir has a major influence on the thermocline depth and thermal stability during the summer season [31]. In this work, due to the lack of the water intake depth operation log, there is limited information on the water intake depth or targeted temperature for water withdrawal. Therefore, the water intake was set to a fixed depth of 5 m below the water surface according to the water intake structure, with water intake windows at every 5 m. Fixing the water withdrawal depth ignores the impact of the dynamic withdrawal depth on the vertical heat distribution within the lake water column. Given the large volume of Advancetown Lake compared with daily water withdrawals, such an impact could be considered minor [35], but there may still be important changes in stratification. During winter, the position of the water offtake may move downward. As shown in Table 5, the impact of increasing the withdrawn volume with a fixed intake depth varies among the climate scenarios in terms of the stability of the water column. The water intake depth might be a source of uncertainty in mimicking the hydrodynamics in Advancetown Lake, but the current model configuration simulated the water temperature distribution reasonably well.

In this work, the catchment output from a previous SWAT study was used as the hydrological input boundary condition for the coupled GLM-AED lake model, and the ecological module was manually calibrated. The lack of water quality sampling data from the hypolimnion meant that nutrient (ammonium and phosphate) release parameters for the bottom sediment may not be especially reliable. These sediment-water fluxes were adopted using relatively small values from the parameters listed in Table 1. The coupled model simulated the ammonium peak in the epilimnion after winter turnover, as shown in

Figure 4a. Increased water quality monitoring and direct measurements of sediment fluxes could improve the simulation accuracy of the lake model and understanding of nutrient cycles in Advancetown Lake.

4.2. Challenges of Water Resource Management

The long-lasting Millennium Drought brought serious challenges to public water supply in the SEQ region during the period from the late 1990s to the early 2000s. As such, emergency legislation and new investments were developed to ensure water supply security. Under a changing climate with more extreme events in the future, together with increasing water withdrawal due to population growth, there may be increased chance of low water storage, which may result in elevated trophic status.

Studies have shown that water level decline caused by drought will reduce the stability of thermal stratification in lakes and bring more frequent and longer mixing events, potentially changing monomictic behavior to polymictic and warming up the hypolimnion [52]. One of the consequences of polymixis is the resuspension of sediments, leading to reduced water clarity [53], which affects the thermal stratification, surface hydrodynamics, and heat storage of lake water [54]. Nutrients released from the bottom sediments or that are attached to particulate matter, enter the epilimnion through vertical mixing, thereby increasing nutrient concentrations [29] and promoting the growth of phytoplankton [55]. Such an outcome can be found in Advancetown Lake during the winter turnover period, with elevated Chl-*a* concentrations (Figure 4g).

Warming temperatures would likely increase the stability of the water column in Advancetown Lake and prolong anoxic conditions in the hypolimnion (Figure S2). As a consequence, there would be increased sediment release of nutrients, such as ammonium [14] and phosphate [12,13], into hypolimnion. Dissolved inorganic phosphorus [22,56] is especially important and has been associated with increased biomass of cyanobacteria in deep lakes [33]. Warming temperatures will also stimulate phytoplankton growth [8] and potentially be associated with harmful algal blooms dominated by cyanobacteria [57], especially during the summer season [58]. Warming temperatures may impact microbial metabolism, leading to more excretion and the accumulation of organic nutrients in surface water [59]. Increases in water temperature are conducive to the dissolution and mineralization of organic matter, which is likely to increase concentrations of dissolved nutrients in the water (Figure 9f,j) [60,61].

Increasing water withdrawal can decrease the flux of nutrients from the hypolimnion into the upper warm and turbulent water layer [32]. This may be an effective strategy to limit algal blooms during warm seasons [62]. For monomictic and deep Advancetown Lake, increasing epilimnetic withdrawal reduces the S_T of the water column. It is worth noting that studies have shown that Chl-*a* concentrations are highly correlated with TP concentrations [3,63], but no such relationship was demonstrated under increasing water withdrawal from Advancetown Lake, regardless of the climate scenario. Temperature increase is the main factor driving changes in Chl-*a* concentration, except for the late winter mixing period, under future climate change scenarios (Figure 9m–p).

Increasing water withdrawn from the epilimnion slightly shortened the average annual stratification duration, but stratification appeared earlier and ended later (Figure S2), depending on the climate scenario. Under the R88 climate condition, increased water withdrawal shortened the thermal stratification duration but did not stop winter overturn failure. Selective withdrawal depth management during the cold season could increase the duration of winter mixing. Increased withdrawal from the epilimnion during winter directly removes oxygenated surface water. Water withdrawn from the thermocline may enhance vertical mixing [30].

The hydrological response of the Upper Nerang River catchment under future climate change conditions affects the hydrodynamics in Advancetown Lake and tends to moderate changes in stratification duration brought by warming temperatures (Figure S2). These changes in catchment flow and nutrient loads will also impact the water quality in the lake.

The concentrations of TN and TP in discharge from the upstream catchment into the lake are expected to decrease by around 18% and 12%, respectively (Table S2). In comparison, the simulated variations in nutrient concentrations are of smaller magnitude in the surface water of Advancetown Lake than in the inflow, indicating the lake serves to buffer changes in catchment nutrient inputs. Under a high emission scenario of R88, the TN concentration is expected to increase by around 8%, while the change in TP concentration is consistent with that in the inflow.

Decreased nutrient concentrations might not result in lower Chl-*a* concentrations in surface waters, but changes in soluble active phosphorus in particular are important for the growth and community structure of phytoplankton [63]. The aforementioned hydrological study shows that changes in vegetation and soil physical and chemical properties of the upstream catchment will lead to lower sediment and nutrient loads under future climate scenarios (Table S2). The decreased loads of organic matter from the upstream catchment under climate change would result in lower concentrations of colored dissolved organic matter (CDOM) in lake water and better water clarity [64,65]. A lower light extinction coefficient from better clarity means that the incident radiation can penetrate deeper into the water layer, reducing the stability of the water body [54,66] and affecting primary productivity [67].

The warming air temperature under future climate change conditions will not only increase the water temperature in Advancetown Lake but may also result in a higher temperature downstream of the dam. High temperature stress will seriously affect the survival and reproduction of aquatic organisms and may eventually lead to the loss of biodiversity [68,69]. Therefore, greater environmental flow and lower water temperatures are important to support downstream health. Lowering the depth of withdrawal for environmental flow can help support cooler water and reduce heat stress on aquatic organisms in the downstream waters [35]. It should also be noted that hypolimnetic withdrawal will result in less DO in the discharged water, especially during thermal stratification. Maintaining or increasing aeration in the downstream channel may be conducive to alleviating heat stress and maintaining good water quality in the downstream waters under future changing climate conditions [7]. The hypolimnetic withdrawal would potentially weaken the stratification of the water column [70] and decrease the sediment and nutrient fluxes entering the epilimnion during winter turnover mixing [17]. Effects of such water management on epilimnetic nutrient levels and phytoplankton dynamics can reasonably be expected, but they also depend on the withdrawal fluxes.

Water resource management at Advancetown Lake faces many challenges from climate change, population growth, and environmental flow demands. The overall impact on lake hydrodynamics and water quality is complex due to the interaction among these factors. As such, advanced algorithms should be considered to enable operational flexibility for multiple objectives, such as flood mitigation, water supply, and environmental flow [71]. Impacts from frequent and intense extreme weather events also need to be fully evaluated for their potentially large and varied impacts on lake ecosystems under future climate change conditions [72].

5. Conclusions

The present work has combined a catchment model with a one-dimensional lake model (GLM-AED) for simulating the hydrodynamics and water quality in Advancetown Lake in subtropical eastern Australia. The combined model reproduced the hydrodynamics and thermal structure in the lake and showed good consistency with the observed water temperature, DO, and other water quality variables during the baseline period from August 2011 to December 2019. The responses of the hydrodynamics and water quality to warming temperatures, climate change, and increasing water withdrawal associated with population growth were investigated for this lake.

The model results showed the increase in water temperature and extension of thermal stratification could be attributed to the warming air temperature under future conditions.

These variations in precipitation and upstream catchment hydrological outputs could partly offset the impact of warming air temperatures, especially for scenarios under a high emission condition of RCP8.5. The impact of increasing withdrawal from the epilimnion on the stability of the water column is antagonistic to that of climate change. However, whether those impacts on the thickness of the epilimnion and thermocline depth from climate change and water withdrawal are synergistic or antagonistic depends on the scenario (RCP4.5 or RCP8.5). Nevertheless, Advancetown Lake is at risk of winter turnover failures during the 2080s under an emission condition of RCP8.5. Concentrations of TN and TP were simulated to increase under a future warming condition of R48-T. For the combination of climate change conditions and upstream catchment hydrological outputs, nutrient concentrations were simulated to decrease except for the TN concentration under R88 emission scenarios (R88-CC and R88-CE). Under future scenarios, Chl-*a* concentrations were modeled to increase, especially during the period after winter mixing.

Due to the increased water temperatures and prolonged thermal stratification duration under future climate warming, the depth of the hypoxia front was simulated to move towards the lake surface and increase in duration, with greater nutrient release from bottom sediments. As such, water sampling in the hypolimnion should be put on the water resource management agenda for assisting to better understand biogeochemical processes in the lake bottom and to support effective engineering programs to deal with the potential adverse effects of climate change on hydrodynamics and water quality in Advancetown Lake.

Supplementary Materials: The following supporting information can be downloaded at: <https://www.mdpi.com/article/10.3390/w16010151/s1>, Figure S1 Surface area and spillway elevation for Advancetown Lake. The black dashed lines refer to the spillway elevations after dam upgrades. Table S1 Climate change scenarios and lake hydrodynamic responses to warming air temperature (T), climate change and upstream catchment hydrological variations (CC), and an increase of 50% in water withdrawal from CC condition by two future periods of '2050s' (2040–2069) and '2080s' (2070–2099) under emission scenarios of RCP4.5 and RCP8.5, respectively. Table S2 Projected changes in air temperature (Ta), rainfall (PCP), and stream flow (Q) and loads of sediment (SS) and nutrients (TN: total nitrogen, TP: total phosphorus) from Upper Nerang River catchment under climate change conditions of RCP4.5 (R45 & R48) and RCP8.5 (R85 & R88) during two future periods of 2050s and 2080s simulated with the SWAT hydrological model (under review). The green to yellow colour bar refers to a change range of 0–5 °C in Ta while the pink to blue colour bar presents a relative change range from –70% to 70% in rainfall and catchment hydrological outputs under future climate change. Figure S2 Distribution of thermal stratification periods under baseline conditions and different future scenarios regarding warming temperatures, climate change, and increasing water demand over the baseline period from July 2011 to July 2019.

Author Contributions: Methodology, C.D., H.Z. and D.P.H.; Software, C.D. and D.P.H.; Writing—original draft, C.D.; Writing—review and editing, C.D., H.Z. and D.P.H.; Visualization, C.D.; Supervision, H.Z. and D.P.H. All authors have read and agreed to the published version of this manuscript.

Funding: No funding available at this moment.

Data Availability Statement: The data are unavailable due to privacy restrictions.

Acknowledgments: The authors are grateful to Seqwater for providing datasets for model setup and calibration. The first author was supported by an International Postgraduate Research Scholarship administered through Griffith University.

Conflicts of Interest: The authors declare no conflicts of interest.

References

1. Wilson, M.A.; Carpenter, S.R. Economic Valuation of Freshwater Ecosystem Services in the United States: 1971–1997. *Ecol. Appl.* **1999**, *9*, 772–783. [[CrossRef](#)]
2. Adrian, R.; O'Reilly, C.M.; Zagarese, H.; Baines, S.B.; Hessen, D.O.; Keller, W.; Livingstone, D.M.; Sommaruga, R.; Straile, D.; van Donk, E.; et al. Lakes as sentinels of climate change. *Limnol. Oceanogr.* **2009**, *54*, 2283–2297. [[CrossRef](#)] [[PubMed](#)]

3. Bucak, T.; Trolle, D.; Tavşanoğlu, Ü.N.; Çakıroğlu, A.İ.; Özen, A.; Jeppesen, E.; Beklioğlu, M. Modeling the effects of climatic and land use changes on phytoplankton and water quality of the largest Turkish freshwater lake: Lake Beyşehir. *Sci. Total Environ.* **2018**, *621*, 802–816. [[CrossRef](#)] [[PubMed](#)]
4. Jenny, J.-P.; Francus, P.; Normandeau, A.; Lapointe, F.; Perga, M.-E.; Ojala, A.; Schimmelmann, A.; Zolitschka, B. Global spread of hypoxia in freshwater ecosystems during the last three centuries is caused by rising local human pressure. *Glob. Chang. Biol.* **2016**, *22*, 1481–1489. [[CrossRef](#)] [[PubMed](#)]
5. Couture, R.-M.; Tominaga, K.; Starrfelt, J.; Moe, S.J.; Kaste, Ø.; Wright, R.F. Modelling phosphorus loading and algal blooms in a Nordic agricultural catchment-lake system under changing land-use and climate. *Environ. Sci. Process. Impacts* **2014**, *16*, 1588–1599. [[CrossRef](#)] [[PubMed](#)]
6. Klug, J.L.; Richardson, D.C.; Ewing, H.A.; Hargreaves, B.R.; Samal, N.R.; Vachon, D.; Pierson, D.C.; Lindsey, A.M.; O'Donnell, D.M.; Effler, S.W.; et al. Ecosystem effects of a tropical cyclone on a network of lakes in northeastern North America. *Environ. Sci. Technol.* **2012**, *46*, 11693–11701. [[CrossRef](#)]
7. Weber, M.; Rinke, K.; Hipsey, M.R.; Boehrer, B. Optimizing withdrawal from drinking water reservoirs to reduce downstream temperature pollution and reservoir hypoxia. *J. Environ. Manag.* **2017**, *197*, 96–105. [[CrossRef](#)]
8. Ward, N.K.; Steele, B.G.; Weathers, K.C.; Cottingham, K.L.; Ewing, H.A.; Hanson, P.C.; Carey, C.C. Differential responses of maximum versus median chlorophyll-a to air temperature and nutrient loads in an oligotrophic lake over 31 years. *Water Resour. Res.* **2020**, *56*, e2020WR027296. [[CrossRef](#)]
9. Carey, C.C.; Ibelings, B.W.; Hoffmann, E.P.; Hamilton, D.P.; Brookes, J.D. Eco-physiological adaptations that favour freshwater cyanobacteria in a changing climate. *Water Res.* **2012**, *46*, 1394–1407. [[CrossRef](#)]
10. Gudasz, C.; Bastviken, D.; Steger, K.; Premke, K.; Sobek, S.; Tranvik, L.J. Temperature-controlled organic carbon mineralization in lake sediments. *Nature* **2010**, *466*, 478–481. [[CrossRef](#)]
11. Read, J.S.; Hamilton, D.P.; Jones, I.D.; Muraoka, K.; Winslow, L.A.; Kroiss, R.; Wu, C.H.; Gaiser, E. Derivation of lake mixing and stratification indices from high-resolution lake buoy data. *Environ. Modell. Softw.* **2011**, *26*, 1325–1336. [[CrossRef](#)]
12. Schauser, I.; Chorus, I. Water and phosphorus mass balance of Lake Tegel and Schlachtensee—A modelling approach. *Water Res.* **2009**, *43*, 1788–1800. [[CrossRef](#)] [[PubMed](#)]
13. Gächter, R.; Müller, B. Why the phosphorus retention of lakes does not necessarily depend on the oxygen supply to their sediment surface. *Limnol. Oceanogr.* **2003**, *48*, 929–933. [[CrossRef](#)]
14. Beutel, M.W. Inhibition of ammonia release from anoxic profundal sediments in lakes using hypolimnetic oxygenation. *Ecol. Eng.* **2006**, *28*, 271–279. [[CrossRef](#)]
15. Jones, I.D.; Elliott, J.A. Modelling the effects of changing retention time on abundance and composition of phytoplankton species in a small lake. *Freshwater Biol.* **2007**, *52*, 988–997. [[CrossRef](#)]
16. Wüest, A.; Lorke, A. Small-scale hydrodynamics in lakes. *Annu. Rev. Fluid Mech.* **2003**, *35*, 373–412. [[CrossRef](#)]
17. Nürnberg, G.K.; Hartley, R.; Davis, E. Hypolimnetic withdrawal in two North American lakes with anoxic phosphorus release from the sediment. *Water Res.* **1987**, *21*, 923–928. [[CrossRef](#)]
18. Jöhnk, K.D.; Huisman, J.; Sharples, J.; Sommeijer, B.; Visser, P.M.; Stroom, J. Summer heatwaves promote blooms of harmful cyanobacteria. *Glob. Chang. Biol.* **2008**, *14*, 495–512. [[CrossRef](#)]
19. Kanoshina, I.; Lips, U.; Leppänen, J.-M. The influence of weather conditions (temperature and wind) on cyanobacterial bloom development in the Gulf of Finland (Baltic Sea). *Harmful Algae* **2003**, *2*, 29–41. [[CrossRef](#)]
20. Ibelings, B.W.; Vonk, M.; Los, H.F.J.; van der Molen, D.T.; Mooij, W.M. Fuzzy modeling of cyanobacterial surface waterblooms: Validation with NOAA-AVHRR satellite images. *Ecol. Appl.* **2003**, *13*, 1456–1472. [[CrossRef](#)]
21. Hense, I. Regulative feedback mechanisms in cyanobacteria-driven systems: A model study. *Mar. Ecol. Prog. Ser.* **2007**, *339*, 41–47. [[CrossRef](#)]
22. North, R.P.; North, R.L.; Livingstone, D.M.; Köster, O.; Kipfer, R. Long-term changes in hypoxia and soluble reactive phosphorus in the hypolimnion of a large temperate lake: Consequences of a climate regime shift. *Glob. Chang. Biol.* **2014**, *20*, 811–823. [[CrossRef](#)] [[PubMed](#)]
23. Woolway, R.I.; Weyhenmeyer, G.A.; Schmid, M.; Dokulil, M.T.; de Eyto, E.; Maberly, S.C.; May, L.; Merchant, C.J. Substantial increase in minimum lake surface temperatures under climate change. *Clim. Chang.* **2019**, *155*, 81–94. [[CrossRef](#)]
24. Fenocchi, A.; Rogora, M.; Sibilla, S.; Ciampittiello, M.; Dresti, C. Forecasting the evolution in the mixing regime of a deep subalpine lake under climate change scenarios through numerical modelling (Lake Maggiore, Northern Italy/Southern Switzerland). *Clim. Dyn.* **2018**, *51*, 3521–3536. [[CrossRef](#)]
25. Jennings, E.; Jones, S.; Arvola, L.; Staehr, P.A.; Gaiser, E.; Jones, I.D.; Weathers, K.C.; Weyhenmeyer, G.A.; Chiu, C.-Y.; De Eyto, E. Effects of weather-related episodic events in lakes: An analysis based on high-frequency data. *Freshwater Biol.* **2012**, *57*, 589–601. [[CrossRef](#)]
26. Jeppesen, E.; Kronvang, B.; Meerhoff, M.; Søndergaard, M.; Hansen, K.M.; Andersen, H.E.; Lauridsen, T.L.; Liboriussen, L.; Beklioğlu, M.; Özen, A.; et al. Climate change effects on runoff, catchment phosphorus loading and lake ecological state, and potential adaptations. *J. Environ. Qual.* **2009**, *38*, 1930–1941. [[CrossRef](#)]
27. De Senerpont Domis, L.N.; Elser, J.J.; Gsell, A.S.; Husar, V.L.M.; Ibelings, B.W.; Jeppesen, E.; Kosten, S.; Mooij, W.M.; Roland, F.; Sommer, U.; et al. Plankton dynamics under different climatic conditions in space and time. *Freshwater Biol.* **2013**, *58*, 463–482. [[CrossRef](#)]

28. Paerl, H.W.; Huisman, J. Climate change: A catalyst for global expansion of harmful cyanobacterial blooms. *Environ. Microbiol. Rep.* **2009**, *1*, 27–37. [[CrossRef](#)]
29. Me, W.; Hamilton, D.P.; McBride, C.G.; Abell, J.M.; Hicks, B.J. Modelling hydrology and water quality in a mixed land use catchment and eutrophic lake: Effects of nutrient load reductions and climate change. *Environ. Modell. Softw.* **2018**, *109*, 114–133. [[CrossRef](#)]
30. Çalışkan, A.; Elçi, Ş. Effects of selective withdrawal on hydrodynamics of a stratified reservoir. *Water Resour. Manag.* **2009**, *23*, 1257–1273. [[CrossRef](#)]
31. Casamitjana, X.; Serra, T.; Colomer, J.; Baserba, C.; Pérez-Losada, J. Effects of the water withdrawal in the stratification patterns of a reservoir. *Hydrobiologia* **2003**, *504*, 21–28. [[CrossRef](#)]
32. Kerimoglu, O.; Rinke, K. Stratification dynamics in a shallow reservoir under different hydro-meteorological scenarios and operational strategies. *Water Resour. Res.* **2013**, *49*, 7518–7527. [[CrossRef](#)]
33. Bormans, M.; Maršálek, B.; Jančula, D. Controlling internal phosphorus loading in lakes by physical methods to reduce cyanobacterial blooms: A review. *Aquat. Ecol.* **2016**, *50*, 407–422. [[CrossRef](#)]
34. Weber, M.; Bohrer, B.; Rinke, K. Minimizing environmental impact whilst securing drinking water quantity and quality demands from a reservoir. *River Res. Appl.* **2019**, *35*, 365–374. [[CrossRef](#)]
35. Calamita, E.; Vanzo, D.; Wehrli, B.; Schmid, M. Lake modeling reveals management opportunities for improving water quality downstream of transboundary tropical dams. *Water Resour. Res.* **2021**, *57*, e2020WR027465. [[CrossRef](#)]
36. Cheng, Y.; Voisin, N.; Yearsley, J.R.; Nijssen, B. Reservoirs modify river thermal regime sensitivity to climate change: A case study in the southeastern United States. *Water Resour. Res.* **2020**, *56*, e2019WR025784. [[CrossRef](#)]
37. Bertone, E.; Stewart, R.A.; Zhang, H.; O'Halloran, K. Analysis of the mixing processes in the subtropical Advancetown Lake, Australia. *J. Hydrol.* **2015**, *522*, 67–79. [[CrossRef](#)]
38. Hipsey, M.R.; Bruce, L.C.; Boon, C.; Busch, B.; Carey, C.C.; Hamilton, D.P.; Hanson, P.C.; Read, J.S.; de Sousa, E.; Weber, M.; et al. A General Lake Model (GLM 3.0) for linking with high-frequency sensor data from the Global Lake Ecological Observatory Network (GLEON). *Geosci. Model Dev.* **2019**, *12*, 473–523. [[CrossRef](#)]
39. Bruce, L.C.; Frassl, M.A.; Arhonditsis, G.B.; Gal, G.; Hamilton, D.P.; Hanson, P.C.; Hetherington, A.L.; Melack, J.M.; Read, J.S.; Rinke, K.; et al. A multi-lake comparative analysis of the General Lake Model (GLM): Stress-testing across a global observatory network. *Environ. Modell. Softw.* **2018**, *102*, 274–291. [[CrossRef](#)]
40. Hipsey, M.R.; Bruce, L.C.; Hamilton, D.P. *Aquatic Ecodynamics (AED) Model Library Science Manual: DRAFT v4*; The University of Western Australia: Crawley, Australia, 2013.
41. Deng, C.; Zhang, H.; Hamilton, D. Sensitivity of streamflow and nutrient loads to climate induced changes in leaf area index and soil organic carbon in a sub-tropical catchment. *J. Hydrol. Reg. Stud.* **2023**. under revision.
42. Luo, L.; Hamilton, D.; Han, B. Estimation of total cloud cover from solar radiation observations at Lake Rotorua, New Zealand. *Solar Energy* **2010**, *84*, 501–506. [[CrossRef](#)]
43. Winslow, L.; Read, J.; Woolway, R.; Brenttrup, J.; Leach, T.; Zwart, J.; Albers, S.; Collinge, D. Package 'rLakeAnalyzer': Lake Physics Tools (Version 1.11.4.1). 2022. Available online: <https://CRAN.R-project.org/package=rLakeAnalyzer> (accessed on 6 November 2023).
44. Idso, S.B. On the concept of lake stability. *Limnol. Oceanogr.* **1973**, *18*, 681–683. [[CrossRef](#)]
45. Schlabing, D.; Frassl, M.A.; Eder, M.M.; Rinke, K.; Bárdossy, A. Use of a weather generator for simulating climate change effects on ecosystems: A case study on Lake Constance. *Environ. Modell. Softw.* **2014**, *61*, 326–338. [[CrossRef](#)]
46. Soares, L.M.V.; Calijuri, M.d.C.; Silva, T.F.d.G.; de Moraes Novo, E.M.L.; Cairo, C.T.; Barbosa, C.C.F. A parameterization strategy for hydrodynamic modelling of a cascade of poorly monitored reservoirs in Brazil. *Environ. Modell. Softw.* **2020**, *134*, 104803. [[CrossRef](#)]
47. Syktus, J.; Toombs, N.; Wong, K.K.-H.; Trancoso, R.; Ahrens, D. *Queensland Future Climate Dataset—Downscaled CMIP5 Climate Projections for RCP8.5 and RCP4.5*; Terrestrial Ecosystem Research Network: Brisbane, Queensland, Australia, 2020.
48. Queensland Government Statistician's Office. *Queensland Government Population Projections, 2018 Edition: LGAs and SA2s*. 2018. Available online: <https://www.qgso.qld.gov.au/issues/5276/qld-population-projections-regions-reports-local-government-areas-sa2-report-2018-edn.pdf> (accessed on 20 November 2019).
49. Fenocchi, A.; Rogora, M.; Sibilla, S.; Dresti, C. Relevance of inflows on the thermodynamic structure and on the modeling of a deep subalpine lake (Lake Maggiore, Northern Italy/Southern Switzerland). *Limnologica* **2017**, *63*, 42–56. [[CrossRef](#)]
50. Martin, J.L.; Wlosinski, J.H. A comparison of reservoir oxygen predictions from one-and two-dimensional models. *Lake Reserv. Manag.* **1986**, *2*, 98–103. [[CrossRef](#)]
51. Verburg, P.; Antenucci, J.P. Persistent unstable atmospheric boundary layer enhances sensible and latent heat loss in a tropical great lake: Lake Tanganyika. *J. Geophys. Res.* **2010**, *115*, D11109. [[CrossRef](#)]
52. Soares, L.M.V.; Silva, T.F.d.G.; Vinçon-Leite, B.; Eleutério, J.C.; de Lima, L.C.; Nascimento, N.d.O. Modelling drought impacts on the hydrodynamics of a tropical water supply reservoir. *Inland Waters* **2019**, *9*, 422–437. [[CrossRef](#)]
53. Zohary, T.; Ostrovsky, I. Ecological impacts of excessive water level fluctuations in stratified freshwater lakes. *Inland Waters* **2011**, *1*, 47–59. [[CrossRef](#)]
54. Heiskanen, J.J.; Mammarella, I.; Ojala, A.; Stepanenko, V.; Erkkilä, K.-M.; Miettinen, H.; Sandström, H.; Eugster, W.; Leppäranta, M.; Järvinen, H.; et al. Effects of water clarity on lake stratification and lake-atmosphere heat exchange. *J. Geophys. Res. Atmos.* **2015**, *120*, 7412–7428. [[CrossRef](#)]

55. Li, S.; Bush, R.T.; Mao, R.; Xiong, L.; Ye, C. Extreme drought causes distinct water acidification and eutrophication in the Lower Lakes (Lakes Alexandrina and Albert), Australia. *J. Hydrol.* **2017**, *544*, 133–146. [[CrossRef](#)]
56. Sherman, B.; Whittington, J.; Oliver, R. The impact of artificial destratification on water quality in Chaffey Reservoir. *Adv. Limnol.* **2000**, *55*, 15–29.
57. Visser, P.M.; Ibelings, B.W.; Bormans, M.; Huisman, J. Artificial mixing to control cyanobacterial blooms: A review. *Aquat. Ecol.* **2016**, *50*, 423–441. [[CrossRef](#)]
58. Trolle, D.; Hamilton, D.P.; Pilditch, C.A.; Duggan, I.C.; Jeppesen, E. Predicting the effects of climate change on trophic status of three morphologically varying lakes: Implications for lake restoration and management. *Environ. Modell. Softw.* **2011**, *26*, 354–370. [[CrossRef](#)]
59. Sarmiento, H.; Montoya, J.M.; Vázquez-Domínguez, E.; Vaqué, D.; Gasol, J.M. Warming effects on marine microbial food web processes: How far can we go when it comes to predictions? *Philos. Trans. R. Soc. Lond. B Biol. Sci.* **2010**, *365*, 2137–2149. [[CrossRef](#)]
60. Malmaeus, J.M.; Blenckner, T.; Markensten, H.; Persson, I. Lake phosphorus dynamics and climate warming: A mechanistic model approach. *Ecol. Modell.* **2006**, *190*, 1–14. [[CrossRef](#)]
61. Gudasz, C.; Sobek, S.; Bastviken, D.; Koehler, B.; Tranvik, L.J. Temperature sensitivity of organic carbon mineralization in contrasting lake sediments. *J. Geophys. Res. Biogeosci.* **2015**, *120*, 1215–1225. [[CrossRef](#)]
62. Brookes, J.D.; Carey, C.C. Ecology. Resilience to blooms. *Science* **2011**, *334*, 46–47. [[CrossRef](#)]
63. Jeppesen, E.; Søndergaard, M.; Jensen, J.P.; Havens, K.E.; Anneville, O.; Carvalho, L.; Coveney, M.; Deneke, R.; Dokulil, M.T.; Foy, B.O.; et al. Lake responses to reduced nutrient loading—An analysis of contemporary long-term data from 35 case studies. *Freshw. Biol.* **2005**, *50*, 1747–1771. [[CrossRef](#)]
64. Yamashita, Y.; Jaffé, R.; Maie, N.; Tanoue, E. Assessing the dynamics of dissolved organic matter (DOM) in coastal environments by excitation emission matrix fluorescence and parallel factor analysis (EEM-PARAFAC). *Limnol. Oceanogr.* **2008**, *53*, 1900–1908. [[CrossRef](#)]
65. An, S.; Chen, F.; Chen, S.; Feng, M.; Jiang, M.; Xu, L.; Wen, S.; Zhang, Q.; Xu, J.; Du, Y.; et al. In-lake processing counteracts the effect of allochthonous input on the composition of color dissolved organic matter in a deep lake. *Sci. Total Environ.* **2023**, *856*, 158970. [[CrossRef](#)] [[PubMed](#)]
66. Christianson, K.R.; Johnson, B.M.; Hooten, M.B. Compound effects of water clarity, inflow, wind and climate warming on mountain lake thermal regimes. *Aquat. Sci.* **2020**, *82*, 6. [[CrossRef](#)]
67. Thrane, J.-E.; Hessen, D.O.; Andersen, T. The absorption of light in lakes: Negative impact of dissolved organic carbon on primary productivity. *Ecosystems* **2014**, *17*, 1040–1052. [[CrossRef](#)]
68. Heino, J.; Virkkala, R.; Toivonen, H. Climate change and freshwater biodiversity: Detected patterns, future trends and adaptations in northern regions. *Biol. Rev. Camb. Philos. Soc.* **2009**, *84*, 39–54. [[CrossRef](#)] [[PubMed](#)]
69. Rasconi, S.; Winter, K.; Kainz, M.J. Temperature increase and fluctuation induce phytoplankton biodiversity loss—Evidence from a multi-seasonal mesocosm experiment. *Ecol. Evol.* **2017**, *7*, 2936–2946. [[CrossRef](#)]
70. Gaugush, R.F. Mixing event in Eau Galle Lake. *Lake Reserv. Manag.* **1984**, *1*, 286–291. [[CrossRef](#)]
71. Castelletti, A.; Yajima, H.; Giuliani, M.; Soncini-Sessa, R.; Weber, E. Planning the optimal operation of a multioutlet water reservoir with water quality and quantity targets. *J. Water Resour. Plann. Manag.* **2014**, *140*, 496–510. [[CrossRef](#)]
72. Mesman, J.P.; Ayala, A.I.; Adrian, R.; De Eyto, E.; Frassl, M.A.; Goyette, S.; Kasparian, J.; Perroud, M.; Stelzer, J.; Pierson, D.C.; et al. Performance of one-dimensional hydrodynamic lake models during short-term extreme weather events. *Environ. Modell. Softw.* **2020**, *133*, 104852. [[CrossRef](#)]

Disclaimer/Publisher’s Note: The statements, opinions and data contained in all publications are solely those of the individual author(s) and contributor(s) and not of MDPI and/or the editor(s). MDPI and/or the editor(s) disclaim responsibility for any injury to people or property resulting from any ideas, methods, instructions or products referred to in the content.